350

HOW OVERHEAD LINES RESPOND TO LOCALIZED HIGH INTENSITY WINDS

Basic Understanding

Task Force
B2.06.09

June 2008

TF B2.06.09

How Overhead Lines Respond to Localized High Intensity Winds

Basic Understanding

June 2008

ISBN: 978- 2- 85873- 037-7

Contributors

Prof. Ghyslaine McCLURE, Convenor WG B2.06 TF 09 (Canada)

Members of WG B2.06 TF 09:

Dr. Daniel GAGNON (Canada), Dr. Asim HALDAR (Canada), Robert LAKE (New Zealand), Sébastien LANGLOIS (Canada), Dr. Jan ROGIER, Convenor WG B2.06 (Belgium), Prof. Eric SAVORY (Canada), Chris THORN (United Kingdom)

SC B2 Reviewers:

Henry HAWES (Australia), Prof. Ruy MENEZES (Brazil)

Members of CIGRE WG B2.06

Jan ROGIER, WG Convenor (Belgium); Pavel FRONEK, Secretary (Czech Republic)

Regular members:
Hee-sung AHN (Korea); Jarlath DOYLE (Ireland); Koji FUKAMI (Japan); Angel GALLEGO (Spain); Elias GHANNOUM (Canada); Jean-François GOFFINET (Belgium); Robert LAKE (New Zealand); Xi-Dong LIANG (China); Ghyslaine McCLURE, Convenor TF 09 (Canada); Vivendhra NAIDOO (South Africa); Carlos do NASCIMENTO (Brazil); Krzysztof PUT (Poland); Fabien RANCOULE (France); Oswaldo REGIS (Brazil); Lars ROLFSENG (Norway); Erik RUGGERI (USA); Ljiljana SAMARDZIC (Serbia); Sava SKROBONJA (Serbia); Chris THORN (United Kingdom)

Corresponding members:
Svein FIKKE (Norway); Arturo GAJARDO (Chile); Tip GOODWIN (USA); Asim HALDAR (Canada); Trevor JACOBS (Australia); Farid KHADRI (Algeria); Friedrich KIESSLING (Germany); Pierre MARAIS (South Africa); Väino MILT (Estonia); Dzevad MUFTIC (South Africa); João Felix NOLASCO (Brazil); Pekka RIISIÖ (Finland); Sergey TURBIN (Ukraine); Brian WAREING (United Kingdom); George WATT (Canada)

)

How Overhead Lines Respond to Localized High Intensity Winds

Basic Understanding

Content

LIST OF TABLES

LIST OF FIGURES

How Overhead Lines Respond to Localized High Intensity Winds

Basic Understanding

Abstract

How Overhead Lines Respond to Localized High Intensity Winds

Basic Understanding

This Technical Brochure presents a brief overview of the literature on localized High Intensity Winds - such as tornadoes and downdrafts - and their effects on overhead power lines in order to provide a basic understanding of these phenomena from an overhead line design perspective. Simplified load cases are proposed based on the present knowledge in the field, recognizing that improvements will follow current and future research efforts, experimental and numerical simulations, physical observations and field data collection.

Résumé

Comportement des Lignes Aériennes face aux Tempêtes de Vent Locales

Vers une Meilleure Compréhension

Cette Brochure Thématique présente un aperçu de la littérature sur les Tempêtes de Vent Locales, comme les tornades et les rafales descendantes, ainsi que leurs effets sur les lignes aériennes. L'objectif est de fournir une meilleure compréhension de ces phénomènes en vue d'améliorer la conception des lignes aériennes ; des cas de charge simplifiés sont proposés sur base des connaissances actuelles dans le domaine. Il va de soi que des améliorations devront encore être faites suite aux acquis de la recherche basée sur des simulations expérimentales et numériques ou des observations et mesures sur site.

How Overhead Lines Respond to Localized High Intensity Winds

Basic Understanding

Executive Summary

Introduction

Wind loading considered in the design of overhead power lines is currently based on extreme values calculated from synoptic boundary layer wind data according to International Standard IEC 60826 (2003) based on CIGRÉ Technical Brochure No. 178 "Probabilistic Design of Overhead Transmission Lines" (2001). There is growing awareness in the overhead line design community that characteristics of such synoptic winds do not always provide proper design parameters to prevent or explain direct wind-related failures.

There is also reliable evidence that localized High Intensity Winds (HIW), such as tornadoes and downdrafts are sometimes the primary cause of failures of supports and even sometimes transverse line cascades. Localized HIW and their flow properties are now actively studied through computational and small-scale experimental simulations, although they are very difficult to observe and measure in natural conditions. Wind field models of localized HIW may be useful for the definition of appropriate design load cases.

Wind is a serious challenge for the overhead line industry. Several utilities in Australia have reported that 80-100% of all weather-related failures on their overhead power network were due to localized HIW. Many of the HIW-related line failures, in fact most of those attributed to downdrafts, have occurred mostly in the Southern hemisphere, where atmospheric icing loads do not govern the design of supports. This explains why HIW effects on lines have been specifically investigated for the last 15 years in Australia, South Africa, Argentina and Brazil, while tornadoes have been extensively studied in the United States. However, most regions of the world should be concerned with the probability of HIW, while mitigation for those winds should be different from one climate to the other.

At present, CIGRÉ has not recommended any specific overhead line design guidelines to account for various forms of localized HIW. This CIGRÉ Technical Brochure (TB) is a first attempt by Task Force 09 of CIGRÉ Working Group B2.06 "Principles of Overhead Line Design" to suggest such guidelines. The proposed loading cases cover basic scenarios to account for the worst effects of a pre-defined localized HIW storm hitting a line section. It builds on the TB 256 "Current Practices regarding Frequencies and Magnitude of High Intensity Winds" (2004) issued by CIGRÉ Working Group B2.16

"Meteorology for Overhead Lines" (Task Force Leader: Henry Hawes, Australia) and on a recent literature survey. A complete list of references is available in the TB.

Definitions

There is a need to define the concept of **"localized High Intensity Wind"** as used here since several different definitions are found in the literature. We suggest restricting this expression to HIW due to localized storm cells that usually cover such a small footprint area that they are very rarely recorded by anemometers at weather stations. They only go reported due to the observation of material damages or to meteorological radar detection.

A downburst is a strong convective downdraft inducing an outward flow of damaging winds when reaching the ground. The downdraft makes contact with the ground and then spreads outwards, causing severe winds at low altitudes. These events are often associated with thunderstorms.

A tornado is a rotating column of air originating from a convective **cloud**, taking the appearance of a narrow funnel and descending below the base of the cloud, often reaching the ground with devastating consequences.

It is suggested here to use the expression **"localized HIW"** to refer to tornadoes and downdrafts. The basic understanding of the physics of thunderstorms needed to appreciate the wind field models described next is given in the TB.

Wind field models of localized HIW

Wind field models of downdrafts

The analysis of recordings of downdrafts showed that the outflow for both the radial and vertical profiles of the horizontal wind velocity is similar to the well-studied fluid flow model called a "wall jet". In this model, the flow field is compared to a jet of fluid impinging on a flat rigid surface. Other important characteristics observed are the rapid fluctuations in wind directions and the influence of the underlying terrain roughness.

A simplified empirical model of a downdraft that addresses directly the problem of overhead line wind loading is presented in **Figure S.1,** which shows the variation of the magnitude of the horizontal, radial component of the wind speed vector, $\mathbf{V_r}$, as a function of position **r** with respect to the centre of the storm cell. The variation is linear up to a point of maximum velocity ($\mathbf{V_r^{max}}$ at position $\mathbf{r^{max}}$) and then decreases exponentially.

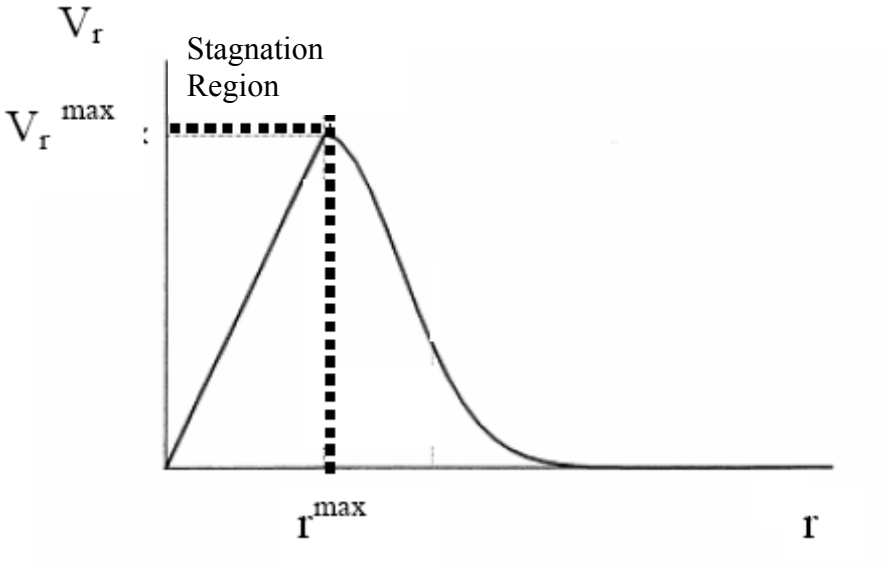

Figure S.1 - Downdraft model: profile of horizontal radial wind speed (Holmes and Oliver, 2000)

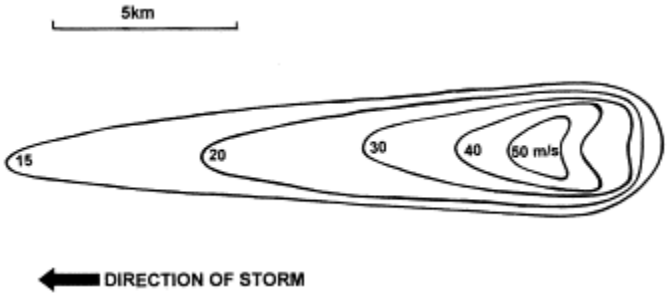

Figure S.2 - Footprint of a downdraft: projection of horizontal radial wind speed (Holmes and Oliver, 2000)

In this model the radial wind speed component is added vectorially to the translational speed of the downdraft centre to give the resultant wind speed representing a significant proportion of the magnitude of the horizontal peak wind speed measured at the front of the downdraft (**Figure S.2**).

From the beginning, one major issue for line design has been to find how the wind speed varies with height during a downdraft. As opposed to the boundary layer winds, downdraft winds reach their maximum intensity at relatively low altitudes. **Figure S.3** shows the variation of high wind speeds with height according to:

- The empirical formula developed by Wood *et al.* (2001);
- The boundary layer wind formula for synoptic winds with terrain roughness exponent 1/7;
- Other profiles obtained from computational simulations by Hangan (2002) with various Reynolds numbers (for different model scales of a real event).

The abscissa of the graph is normalized with respect to the maximum wind speed, $\mathbf{V_{max}}$, and the elevation plotted on the ordinate is normalized with respect to height where the wind speed is at one half of its maximum value, $\mathbf{Z_{0.5*Vmax}}$. The "nose shape" profiles obtained from Wood's model and by more advanced theoretical models predict generally predict higher wind velocities at lower elevations than the exponential boundary layer model.

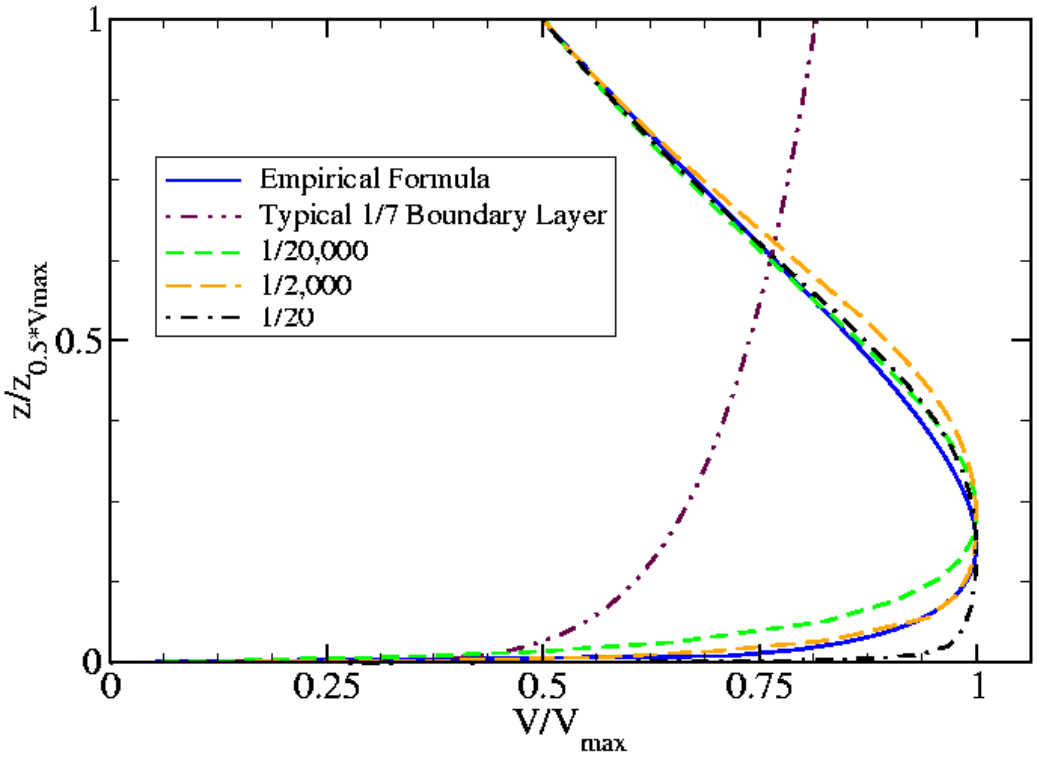

Figure S.3 – Downdraft vertical radial velocity profiles (Hangan, 2002)

Along with computational fluid dynamic simulations, physical reduced-scale simulations in laboratories have been tried. There are also some ongoing research developments on large-scale downburst simulation, suitable for structural model testing. More details about recent developments in downburst wind field models are given in the TB.

Wind field models of tornadoes

Some of the most severe winds that can be produced by thunderstorms occur through tornadoes. In the Southern hemisphere, strong downdrafts produced by thunderstorms are often described by tornadic type winds in terms of their speed, which is similar to the top range of an F2 tornado. According to the Fujita-Pearson scale each tornado can be assigned a number 0 to 5 for each of the following intensity indicators:

- maximum wind speed;
- path length;
- path width.

It is interesting to consider the frequency distribution according to the intensity: for example, designing for the F2 tornado scale would include 86% of events, 58% of which would likely have a path width of 50 m or less, and the remaining 28% would have a path width between 50 m and 160 m.

The general structure of the wind flow field of tornadoes is now well known, although their detailed wind velocity profiles have yet to be quantified and validated. A large part of the basic knowledge on tornadoes was revealed through laboratory simulations. The tornado wind profile model of Wen (1975) illustrated in **Figure S.4** is still used today. The figure represents the relative wind velocity with respect to the centre of the tornado and its decomposition into three orthogonal components: tangential (**T**), radial (**R**) and vertical (**W**). Velocity profiles are developed with respect to elevation above ground (**z**) and radial distance (**r**) from the centre of the tornado. The direction and speed of the centre of the tornado will affect the maximum wind speeds.

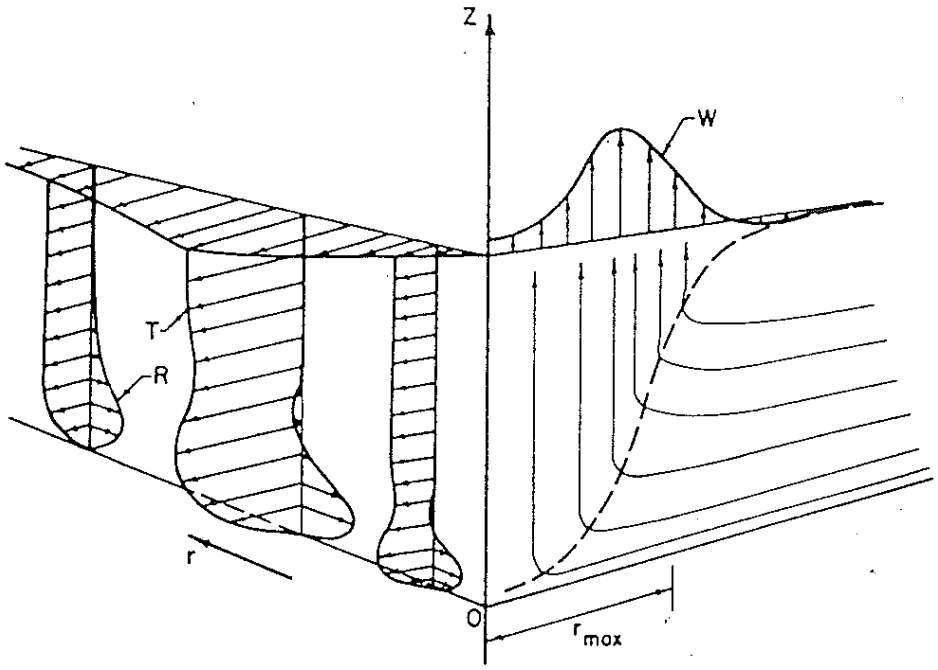

Figure S.4 - Schematic wind field in a tornado vortex (Wen, 1975)

Risk assessment of localized HIW events

When, where and how often do localized HIW occur? How severe are they? Those questions have proven to be difficult to answer. Most electric utilities – except in the United States and Argentina (for tornadoes), in Australia, Argentina and South Africa (for downdrafts) – have limited information available on wind speeds in tornadoes and downdrafts. In the absence of sufficient information, only a deterministic approach may be adopted. Risk models for downdrafts and tornadoes are presented in the TB.

Effects of localized HIW on overhead lines

Effects of downdrafts

Downdrafts can sometimes be larger than tornadoes in extent, i.e. more than one span can be affected by an event. Downdraft wind loading varies greatly depending on the development stage at the moment the structure is hit. If a downdraft is close to touch down, high downward vertical winds are expected, but after touch down, the load is mainly horizontal with possibly some upward vertical load due to the formation of a ring vortex. Evidence of high wind shears above ground boundary layer has also been collected in many cases. Recent work has used computational fluid dynamics models to generate time histories of turbulent wind velocity profiles suitable for dynamic analysis of structures. Results obtained so far indicate that static effects dominate the response of towers.

Effects of tornadoes

For a classical lattice tower with inclined main legs, the intersection of the main tower legs (**Figure S.5a**) is usually selected to coincide nearly with the horizontal resultant of the total synoptic wind load on tower and conductors in order to minimize the stresses in the bracing members between the main tower legs. If the wind load on the conductors is neglected, due to the rotation and the assumed very narrow path of a tornado, the resultant wind load will be lowered so that the bracing members could be overstressed. If buckling of one of those bracings occurs, the tower may fail in a shearing mode. This failure mechanism is often observed for structures suffering a very narrow HIW storm gust such as during a tornado. Some tower structures have also been observed to have failed in a torsional mode during such events, which may have resulted from the sequence of failure of their members rather than from direct torsional loading.

Transverse cascades

Transverse cascades of overhead lines are almost exclusively initiated by HIW and large synoptic wind storms. When a support falls in the transverse direction, its adjacent effective spans become longer and large conductor tensions are induced at the adjacent structures, creating significant transverse and longitudinal load imbalances. If these supports also fail, the collapse may progress, forming a transverse cascade. During major wind storm such as tropical cyclones, hurricanes, typhoon and extra-tropical storms it is to be expected that multiple failures of a line occur due to the potential for multiple closely-spaced HIW gusts, thus increasing the potential for triggering transverse cascades.

Overview of localized HIW-resistant design provisions

The most elaborate downdraft loading model is found in the Australian ENA C(b)1: 2006. This document is being reviewed during 2007-2008 and will be incorporated into an Australian / New Zealand design standard. It will provide for more defined downdraft wind regions as well as synoptic wind regions and their respective span reduction factors, wind velocities and related loadings. Tornado wind loadings for F2 events are provided and will be only a requirement for major inter regional lines.

ASCE Manual 74 (1991) and its draft 2005 revision provide many useful information on localized HIW, especially on tornadoes. The approach for tornado-resistant design is to consider a uniform wind speed corresponding to a moderate tornado scale F1 or F2 applied only to the transmission structure over the full structure height from any direction. For a small microburst, it is suggested to use the same load as for the tornado.

Although the main focus of the CIGRÉ TB 256 (2004) was to describe the characteristics of all major types of HIW storms, it also made some recommendations in relation to the spatial effects of wind gust types. For regions prone to tornadoes, it suggested that line supports should be designed to resist a uniform F2 tornado wind speed coming from any direction and a rotational wind with no loads on the conductors. For downdrafts, it recommended that the full uniform wind be applied on both the structures and the supported conductors. The TB 256 also recommended that span reduction factors such as used with synoptic winds be ignored since narrow wind gusts are well correlated horizontally.

Proposed simplified loading cases for localized HIW

This TB is proposing simplified loading cases which are summarized in **Table S.1**. They cover six basic scenarios to account for the worst effects of a pre-defined localized HIW storm hitting a line section: five loading cases for downbursts and one multi-directional loading case for tornadoes.

These loading cases are meant to provide a conservative estimate of the response of the target support to localized HIW with consideration of the wind load path. They are determined from a uniform wind velocity profile without correction for height, gust effect, span length, terrain roughness and topography. Except for the partial support loading for downdrafts (Patch load cases DPB and DPA), which is specific to lattice towers with inclined legs and guyed supports, all the loading cases indicated in Table S.1 are applicable to all types of line supports. As indicated in the last column of the table, several of these loading cases have already been developed or used (as is or with modifications).

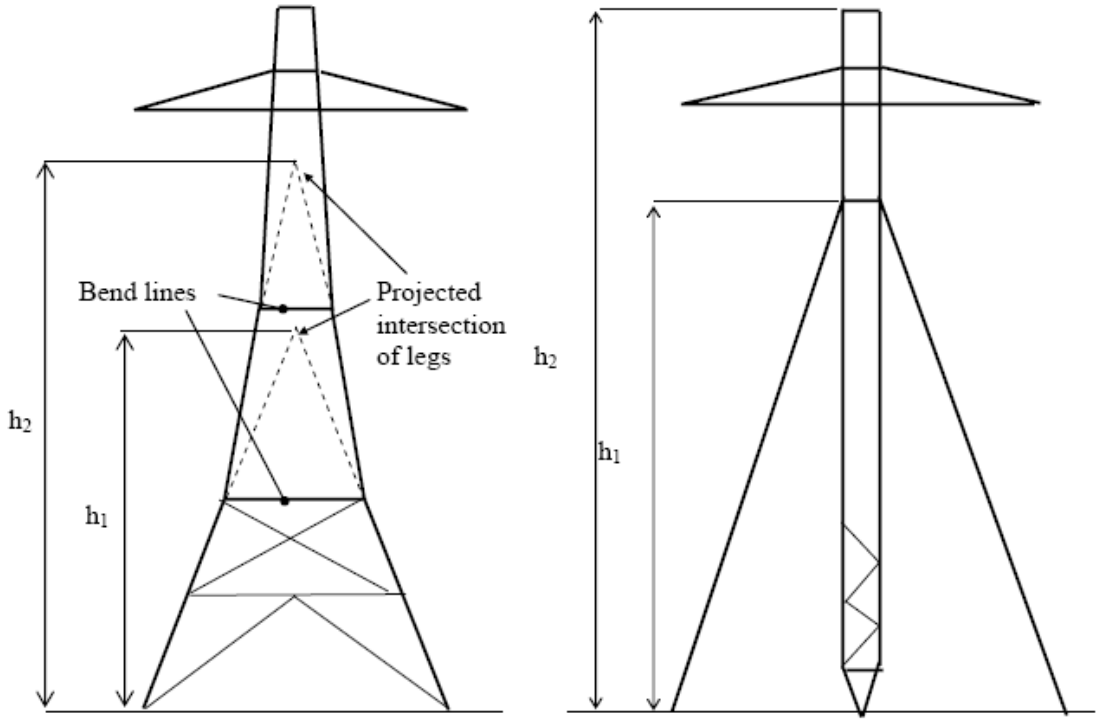

a) Self-supporting tower **b) Guyed structure**

Figure S.5 - Schematic support geometries for localized HIW loading cases

Table S.1 - Design loading cases for localized HIW

	HIW load case	Horizontal wind direction	Wind on		Also developed or used by
			conductor	support	
Downdraft	DT	Transverse	yes	Full height – all types of supports	ENA Australia
	DL	Longitudinal			
	DO	Oblique			
	DPB	Transverse and longitudinal	no	Below h_i for lattice tower (i = 1, 2, …)	Exclusive to CIGRÉ (Figure S.5 a & b)
				Below h_1 for guyed structure	
	DPA	Transverse and longitudinal	yes	Above h_1 for guyed structure	ENA Australia
Tornado	T(φ)	Multidirectional: φ = 0°, 45°, 90°	none	Full height – all types of supports	Eskom South Africa
					Hidronor (Transener) Argentina
					ASCE Manual 74 & HydroOne Canada (weightless conductors)

Conclusions

In many regions of the world not exposed to atmospheric icing, localized High Intensity Winds pose the greatest risk to failure of overhead lines. However, only a few countries have put in place codified procedures that provide a level of mitigation of the effects and provide increased security of overhead lines. In other regions where localized HIW events now appear to be more frequent than previously anticipated, utilities are looking at simple ways of reducing the risk of catastrophic failures.

Some simplified design loading cases are proposed in this Technical Brochure to account for the effects of localized High Intensity Winds on overhead line supports. They are recommended for use by utilities without codified procedures in place.

How Overhead Lines Respond to Localized High Intensity Winds

Basic Understanding

1. Introduction

Wind is a serious challenge for the overhead distribution and transmission line industry. According to Dempsey and White (1996), several utilities in Australia have reported that 80-100% of all weather-related failures on their overhead power network were due to localized **High Intensity Winds** (HIW), such as tornadoes and convective downdrafts. Many of the HIW-related line failures, in fact most of those attributed to downdrafts, have occurred mostly in the Southern hemisphere, where atmospheric icing loads do not govern the design of supports. This explains why HIW effects on lines have been specifically investigated for the last 15 years in Australia, South Africa, Argentina and Brazil, while tornadoes have been extensively studied in the United States.

There is reliable evidence (Nolasco, 1996 and CIGRÉ WG B2.06, 2007) that localized HIW are sometimes the primary cause of failures of overhead lines in countries that do not have codified design procedures to account for HIW-related loads. In such cases, localized HIW hit lines in off-design conditions, i.e. they apply loads that are more critical than those considered in design, causing failures of overhead line supports and even sometimes catastrophic transverse line cascades.

Most wind-resistant design codes and practices for constructed facilities, including the International Standard IEC 60826 (2003) for overhead power lines, are based on synoptic winds (CIGRÉ WG 22.06, 2001 and CIGRÉ WG B2.06, 2006). Typically, extreme wind pressures are calculated based on wind speeds extrapolated from wind speeds recorded at weather stations that generally affect a large area and exhibit conventional characteristics. Synoptic winds are idealized as essentially horizontal winds with a vertical velocity profile described by the boundary layer theory and its well known power law where the value of the exponent depends on terrain roughness.

Flying debris from buildings and vegetation generated by tornadoes and downdrafts can cause significant damage to overhead lines. Distribution lines are especially at risk as most building structures and vegetation that are stripped are within 10 m of the ground and are blown horizontally. It is not possible to quantify the probability of line failure associated to such debris and projectiles, although strict maintenance management of surrounding vegetation may contribute to reduce it. Such failures are considered as accidental and are best addressed in global design considerations for line security. This Technical Brochure therefore considers the direct effects of wind pressures on the overhead line.

After presenting useful definitions in **Section 2**, **Section 3** of this Technical Brochure summarizes our current knowledge on wind field models of localized HIW. Their flow properties are actively studied through computational and reduced-scale experimental simulations, although they are very difficult to observe and measure in natural conditions (Wood *et al*., 2001; Letchford *et al*., 2002; Hangan, 2002; Brooks *et al*., 2003; Mason *et al*., 2006; Chay and Albermani, 2004; Chay *et al.*, 2006).

Risk assessment of those wind events is also of great interest to the distribution and transmission line industry and is the subject of **Section 4** (Milford and Goliger, 1997; Goliger and Milford, 1998; Li, 2000; Oliver *et al*., 2000).

Section 5 addresses the effects of localized HIW storms on overhead lines, while **Section 6** summarizes existing design provisions, guidelines or applications. Some electric utilities in Argentina, South Africa, and Canada have developed or used simplified loading models to account for the possibility of a tornado striking a line (Behncke and White, 1984; Behncke *et al*., 1994; Ishac and White, 1995; Behncke and White, 2006). Also, the American Society of Civil Engineers (ASCE) Manual 74 (1991) contains design guidelines against HIW with recent refinements in the 2005 draft revision, the main focus being again on tornado-resistant design. On the other hand, Australian standards (Electricity Networks Association [ENA], 2006) are more specific for downburst loadings: these design provisions are currently under review (in 2007) and will be incorporated into an Australian/New Zealand design standard.

At present, CIGRÉ has not recommended any specific overhead line design guidelines to account for various forms of localized HIW. **Section 7** of this document is a first attempt by CIGRÉ Working Group B2.06 “Principles of Overhead Line Design” to recommend such guidelines. It builds on the work presented in 2004 by CIGRÉ Working Group B2.16 (Technical Brochure 256) on meteorological aspects, frequency and amplitude of HIW and on a recent literature survey prepared by Langlois (2006) for the Task Force 09 of WG B2.06. The proposed loading cases cover six basic scenarios to account for the worst effects of a pre-defined localized HIW storm hitting a line section: five loading cases for downdrafts and one multi-directional loading case for tornadoes. They are recommended for use by utilities without a codified procedure in place for HIW-resistant design. Utilities in Australia, New Zealand, Argentina, South Africa, USA, etc. who already have specific design procedures are expected to go beyond these simplified loading cases if they find them inadequate.

Important practical limitations of the proposed loading cases are stated in **Section 8** with ensuing research and observation needs.

Four example case studies are included in **Appendix A**, which illustrate the use of several localized HIW loading cases for line sections with self-supporting lattice towers that were not originally designed to resist such effects. Results are compared with those obtained with loading cases using the synoptic wind loading method of International Standard IEC 60826. These case studies are excerpts from Langlois (2007).

Appendix B gives the detailed parameters of the numerical wind models of Wood for the downdrafts and Wen for the tornadoes, as used by Langlois (2007).

Appendix C provides some synoptic tables indicating the influence of the direction and height of both tower and conductor wind load on the internal forces in the main legs and bracing members of a tangent suspension lattice tower.

2. Definitions

There is a need to define the limits of the concept of **"localized High Intensity Wind"** as used here since several different definitions are found in the literature. We suggest restricting this expression to High Intensity Winds (HIW) due to **localized storm cells** that usually cover such a small footprint area that they are very rarely recorded by anemometers at weather stations. They only go reported due to the observation of material damages or to meteorological radar detection. For the purpose of this Technical Brochure, we further suggest designating five categories of winds:

- Synoptic winds;
- Major tropical storms;
- Sub tropical thunderstorms;
- Downbursts;
- Tornadoes.

Synoptic winds are those associated with large moving pressure systems and usually cover hundreds or thousands of kilometers.

Major tropical storms such as hurricanes, typhoons, cyclones and extra-tropical storms will not be covered in the proposed simplified loading cases for line design.

Sub tropical thunderstorms are convective storms in sub tropical regions that occur within frontal systems and that can have embedded destructive wind cells. These cells can form severe downdrafts and tornadoes, which can also occur in isolation.

A downburst is a strong convective downdraft inducing an outward flow of damaging winds when reaching the ground. The downdraft makes contact with the ground and then spreads outwards, causing severe winds at low altitudes. These events are often associated with thunderstorms because they involve thermal convection (See Section 3) but they can occur without precipitation or lightning. In the literature, downdrafts are further divided into macrobursts (more than 4 km of high velocity wind front) and microbursts (less than 4 km). However, such a refined classification is not necessary for overhead line design as most downdrafts have a wind front dimension exceeding typical wind spans.

A tornado is a rotating column of air originating from a convective cloud, taking the appearance of a narrow funnel and descending below the base of the cloud, often reaching the ground with devastating consequences.

It is suggested here to use the expression **"localized HIW"** to refer to tornadoes and convective downdrafts (i.e. downbursts of various sizes). Several authors, including Behncke et al. (1994), Dempsey and White (1996), and Savory *et al*. (2001), accept a similar definition.

3. Wind field models of localized HIW

3.1 General

A general understanding of the physics of thunderstorms is needed to appreciate the wind field models described next. The instability of the air, caused by cold air over a warm surface, generates a convection where warm moist air rises from the ground (updraft) and is substituted by dry colder air from aloft (downdraft). Due to adiabatic cooling the rising air becomes saturated and the water vapor condenses into the convective clouds. The updraft is usually strengthened due to the release of latent heat during condensation.

As illustrated schematically in **Figure 1**, the **thunderstorm process** is divided into three stages (Battan, 1984):

- the cumulus stage;
- the mature stage;
- the dissipating stage.

During the cumulus stage, several cumuli clouds converge and combine, forming a large cell with precipitation particles. This formation is dominated by updrafts. That moist air can ascend up to several kilometers. As it cools down and loses its buoyancy, a downdraft is initiated. This is the beginning of the mature stage during which both strong updrafts and downdrafts are present. The dissipating stage is characterized by a weak downdraft and the dissipation of the storm cell.

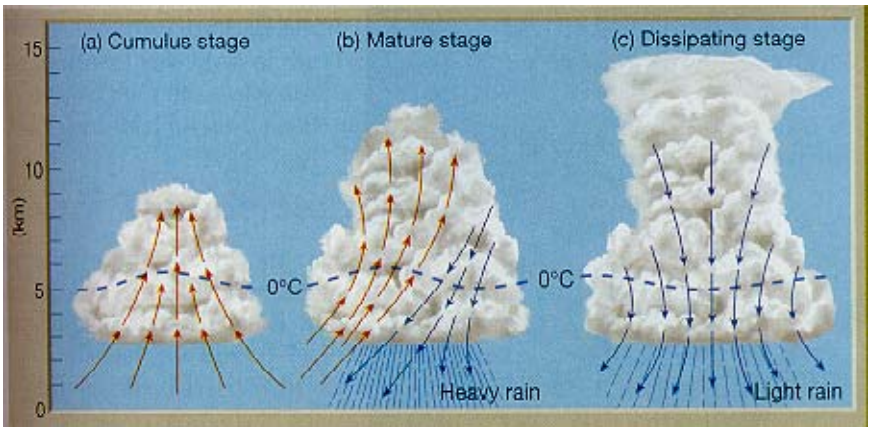

Figure 1 - The three stages of a thunderstorm (Lutgens and Tarbuck, 2001)

Two types of storm cells are the ordinary cell and the super cell (CIGRÉ WG B2.16, 2004). The latter covers a larger area and can produce the most devastating of all thunderstorm wind event, the tornado. The downdraft part can also produce high velocity winds as it reaches the ground. When this mechanism is strong enough, it is called a downburst. In general, severe wind storms last for one to three hours and the storm cell travels at 20 to 40 km/h – some storms also develop multiple cells. As the storm cell

translates, HIW will rarely last more than 15 minutes at a particular location (Hawes and Dempsey, 1993). Much is still to be learned from the wind field of thunderstorms. Letchford *et al*. (2002) summarize the extent of the research done on the subject prior to 2002 and outline the most important characteristics of thunderstorm winds, and differentiate them from synoptic winds. The main differences are:

- their non-stationary nature;
- their complex three-dimensional flow pattern;
- their velocity profile with height;
- the lesser role of turbulence;
- their smaller spatial and temporal extents.

Tornadoes originate from the updraft part of the storm cell.

3.2 Downdrafts

3.2.1 General

Fujita (1981, 1990) described a downburst as a strong downdraft which induces an outward flow of damaging winds on or near the ground. The downdraft makes contact with the ground and then spreads outwards, causing severe winds at low heights. The lifetime of a downburst is generally between 5 and 30 minutes for a macroburst and between 5 to 10 minutes for a microburst (McCarthy and Melsness, 1996). It is noteworthy that the maximum downburst wind speed ever recorded is 67 m/s in 1982 at Andrews Air Force Base near Washington, D. C. (Li and Holmes, 1995).

Following Fujita's observations, three important projects were initiated in the United States to collect meteorological data on downbursts:

- the Northern Illinois Meteorological Research on Downbursts (NIMROD) in 1978;
- the Joint Airport Weather Studies (JAWS) in 1982;
- the Microburst and Severe Thunderstorm (MIST) Project in 1986.

Observations indicate that the passage of a downburst generally creates two distinct peaks in the time history of horizontal wind speed; these two peaks suggest that the wind speed in the center of the downburst is small and that it increases with radial distance up to a certain limit. (Letchford *et al*., 2002)

Hjelmfelt (1988) presented a detailed analysis of microbursts recorded during the JAWS project. He characterized the size of those events and concluded that the outflow was similar to the well-studied fluid flow model called a "wall jet" for both the radial and vertical profiles of horizontal wind velocity. In this model, the flow field is compared to a jet of fluid impinging on a flat rigid surface. Other important characteristics observed are the rapid fluctuations in wind directions during the passage of the storm and the influence of the underlying terrain roughness (Holmes, 1999 and 2001).

3.2.2 The wall jet model

When performing early numerical simulations, meteorologists were often interested in the whole process of convective downdrafts and did not focus on the distribution of high winds near the ground. From a structural engineering point of view, however, damaging winds are better represented by the wall jet model.

The first numerical simulation using the wall jet model to describe low-altitude wind flow over objects was performed by Selvam and Holmes (1992). More recently, Holmes and Oliver (2000) developed a simplified empirical model of a downburst that addresses directly the problem of overhead line wind loading.

Figure 2 is a schematic graph showing the variation of the magnitude of the horizontal, radial component of the wind speed vector, $\mathbf{V_r}$, as a function of position **r** with respect to the centre of the storm cell. The variation is linear up to a point of maximum velocity ($\mathbf{V_r^{max}}$ at position $\mathbf{r^{max}}$) and then decreases exponentially. In their model this component is then added vectorially to the translational speed of the downburst centre to give the resultant wind velocity. This translational speed can represent a significant proportion of the magnitude of the horizontal peak wind speed measured at the front of the downburst. This effect is illustrated in **Figure 3**.

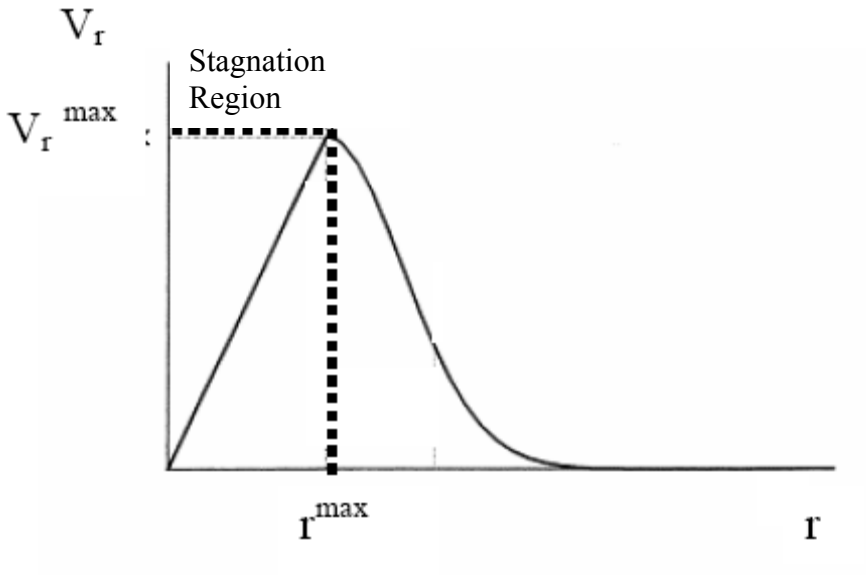

Figure 2 - Downburst model: profile of horizontal radial wind speed (Holmes and Oliver, 2000)

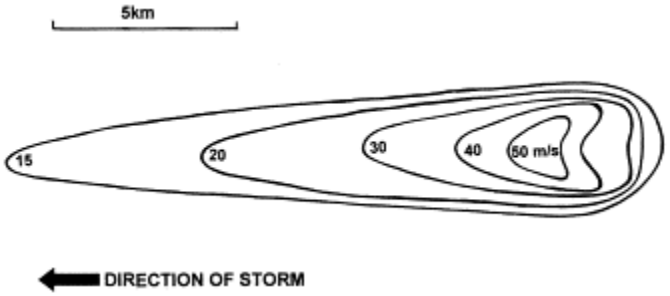

Figure 3 - Footprint of a downburst: projection of horizontal radial wind speed (Holmes and Oliver, 2000)

3.2.3 Vertical profile

From the beginning, one major issue has been to find how the wind speed varies with height during a downburst. This is certainly a very important issue for overhead line design since high or low wind speed assumptions on the supported conductors lead to very different loading patterns on the line supports.

As opposed to the boundary layer winds, downburst winds reach their maximum intensity at relatively low altitudes. In general, the vertical profile shows a peak between 50 and 100 m above ground (Holmes, 1999). Early observations by Fujita and Hjelmfelt during the 1980s are among the very few full-scale measurements available to verify the vertical profiles. Work by Wood *et al*. (2001) gives an empirical formula to approximate the distribution of high wind speeds with height: this simplified model is presented in more details in Appendix B.

Figure 4 shows the difference between:

- this empirical formula of Wood *et al.* (2001);
- the typical boundary layer wind formula with terrain roughness exponent 1/7;
- other profiles (representing different model scales of a real event and, hence, different Reynolds numbers) obtained from computational fluid dynamic simulations of a downburst performed by Hangan (2002).

The abscissa of the graph is normalized with respect to the maximum wind speed, $\mathbf{V_{max}}$, and the elevation plotted on the ordinate is normalized with respect to height where the wind speed is at one half of its maximum value, $\mathbf{Z_{0.5*Vmax}}$. It should be noted that these simulations and the formula of Wood *et al.* (2001) are for steady, continuous, impinging jets, rather than the more realistic case of a transient, time-varying event within which the velocity profile shape at any location also varies greatly with time. It appears that the "nose" of the transient jet profile at the time of maximum wind speed is flatter than in the steady jet case shown here.

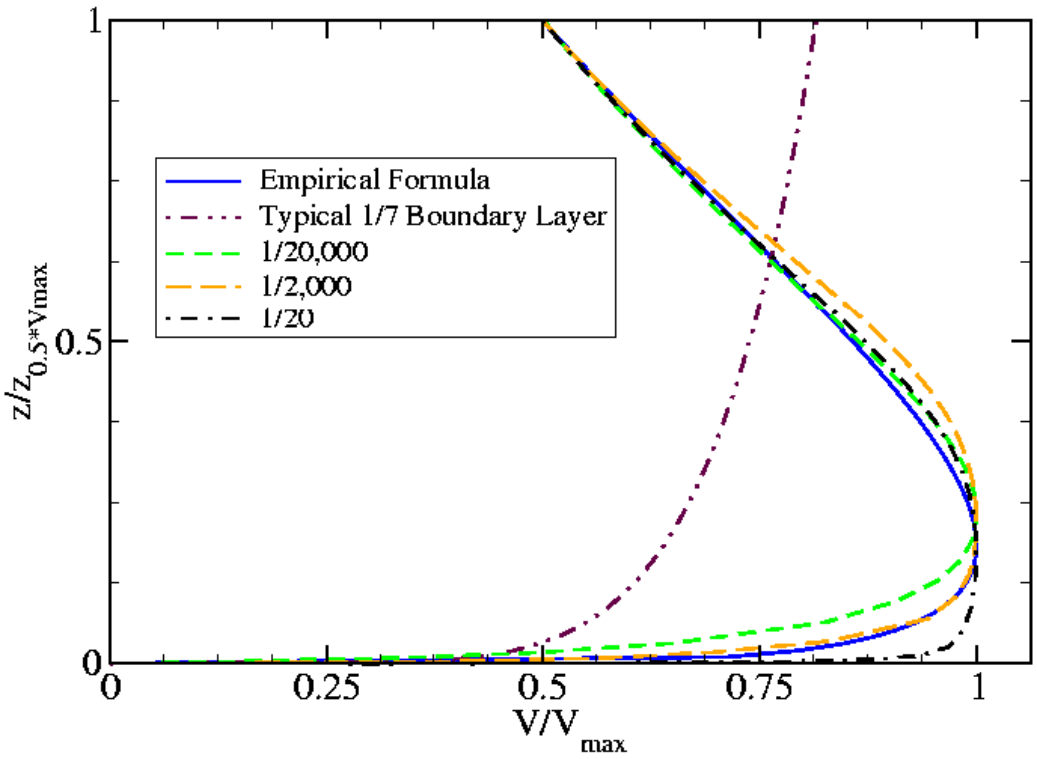

Figure 4 - Downburst vertical radial velocity profiles (Hangan, 2002)

Until very recently, Computational Fluid Dynamics (CFD) models of downbursts assumed simple momentum jets, whereas the real events are density driven, involving time-varying thermodynamic processes that are not accounted for in the numerical models. Another challenge is to generate, from those simulations, realistic wind loads applicable to structures, i.e. with appropriate frequency content and duration. This has been attempted by Chay and Albermani (2004 & 2005) and recently by Chay *et al.* (2006) who have developed a time-varying downburst model suitable for the generation of turbulent wind loads in a dynamic structural analysis.

The work by Hangan (2002) (**Figure 4**) provides another CFD-based numerical downburst model which has been used to generate non-turbulent quasi-static loads on line supports by Shehata (2006).

Wood *et al*. (2001) have simulated a downburst using an outlet jet from a wind tunnel impinging on a vertical board. The method represents well the velocity profiles but fails to demonstrate the transient characteristics of the flow (Holmes, 2001). One major problem is that the source, contrary to a real storm, is stationary. In reality, the flow characteristics of the back flow may prove important in the development of a horizontal vortex roll, which further complicates the pressure field on the conductors as the downburst translates. Recent progress includes the development of a moving jet method by Mason *et al.* (2005) in Texas. There are also ongoing research developments on large-scale, physical downburst simulation, suitable for structural model testing, at the Boundary Layer Wind Tunnel Laboratory of the University of Western Ontario in

Canada (Lin *et al.*, 2006, Lin and Savory, 2006). It should be recognized that physical reduced-scale simulations in laboratories are still very limited and do not compare to the well-developed boundary layer wind tunnel work. Nor are such experiments conducted on a large enough physical scale to allow for testing of models of structures such as towers.

3.3 Tornadoes

3.3.1 General

Some of the most severe winds that can be produced by thunderstorms occur through tornadoes. In the Southern hemisphere, strong downdrafts produced by thunderstorms are often described by tornadic type winds in terms of their speed, which is similar to the top range of an F2 tornado.

The visible shape of the tornado (which makes it much more identifiable than the "invisible" convective downdraft) is mostly due to the presence of water droplets. The width of path of damaging winds in tornadoes is generally smaller than a few hundred meters, and rarely reaches one kilometer (Battan, 1984). It is fair to say that a tornado hitting a line support would also typically induce strong wind pressures on the supported conductors on a fraction of the wind span. However, realistic consideration of the conductor loads may be too complex for simplified design load cases. Path lengths of tornadoes vary according to their strength and can exceed 50 km (Holmes, 2001).

The most widely used tornado intensity scale is called the Fujita-Pearson (FPP) scale (Fujita, 1973). Each tornado can be assigned a number between 0 and 5 for each of the following intensity indicators:

- maximum wind speed;
- path length (along the direction of propagation);
- path width (perpendicular to the direction of propagation).

These gust wind speeds were derived from qualitative assessment of observed damages. ASCE Manual 74 (2005) states that they are equivalent to the "fastest-quarter-mile" wind speeds assumed at 15-30 feet above ground. For simplicity, however, it is common practice to characterize tornadoes based only on wind speed and the intensity scale varies between F0 and F5.

The different ranges of the original Fujita-Pearson scale are given in **Table 1**. This classification was based on 24.930 events recorded from 1950 to 1971 (Fujita, 1971& 1973) and data on path width were introduced a few years later by Pearson (Fujita and Pearson, 1972). Expected damages qualified in the table refer to constructed facilities in general and most likely to buildings.

It is interesting to consider the frequency distribution of these events: for example, designing for the F2 tornado scale (maximum wind speed of 70 m/s) would include 86.1 % of events, 57.6 % of which would likely have a path width of 50 m or less and another 28.5 % a width of no more than 160 m, i.e. somewhere between 50 m and 160 m.

Table 1 - The Fujita-Pearson tornado scale

F Scale	Maximum wind speed (m/s)	Path length (km)	Path width (m)	Expected damages	Frequency distribution (%)	Cumulative frequency (%)
0	< 33	< 1.6	< 15	light	22.9	22.9
1	50	1.6-5.0	15-50	moderate	34.7	57.6
2	70	5-16	50-160	considerable	28.5	86.1
3	92	16-50	160-500	severe	10.7	96.8
4	116	50-159	500-1600	devastating	2.7	99.5
5	142	159-507	1600-5000	incredible	0.5	100

On February 1, 2007, the Fujita scale has been updated to the Enhanced Fujita Scale (EF Scale – **Table 2**) for operational use by the National Weather Service in the United States. (McDonald and Mehta, 2006)

Table 2 - The Enhanced Fujita tornado scale (McDonald and Mehta, 2006)

Original F Scale	Maximum wind speed (m/s)[1]	New EF Scale	Maximum wind speed (m/s)
0	< 33	0	< 38
1	50	1	49
2	70	2	60
3	92	3	74
4	116	4	89
5	142	5	> 90

The EF Scale was introduced to provide a better correlation between observed damage and wind speed by means of 28 specific damage indicators accounting for different degrees of damage that occur with different types of structures. In particular, Damage Indicator (DI) no. 24 of the EF Scale relates to electrical overhead lines. The typical constructions of this indicator include the following:

- single wood poles with wood cross arms;
- single steel or concrete poles with metal cross arms;
- metal trussed towers.

Six Degrees of Damage (DOD) are categorized as listed in **Table 3** for this DI. This classification indicates that the EF3 tornado scale (maximum wind speed of 74 m/s) corresponds to suitable wind speed design values for overhead lines.

[1] Wind speed corresponding to the 3-s gust.

Table 3 – Degrees of Damage (DOD) in Electrical Overhead Lines according to the EF tornado scale (McDonald and Mehta, 2006)				
DOD	Damage description	Maximum wind speed (m/s)		
		Expected value	Lower Bound	Upper Bound
1	Threshold of visible damage	37	31	44
2	Broken wood cross member	44	36	51
3	Wood poles leaning	48	38	58
4	Broken wood poles	52	44	63
5	Broken or bent steel or concrete poles	62	51	67
6	Collapsed metal truss towers	63	52	74

The general structure of the wind flow field of tornadoes is now better known, although their detailed wind velocity profiles have yet to be quantified and validated. A large part of the basic knowledge on tornadoes was revealed through laboratory simulations although today research using computational modeling is dominant. A comprehensive review of the evolution of physical modeling of tornadoes is available in Letchford *et al*. (2002).

3.3.2 The Wen tornado model

The tornado wind profile model illustrated in **Figure 5** was developed by Wen (1975) and is still used today. Detailed equations are given in **Appendix B**.

Figure 5 represents the relative wind velocity with respect to the centre of the tornado since it does not include the translational velocity of the tornado itself. The wind velocity vector is decomposed into three orthogonal components: tangential (**T**), radial (**R**) and vertical (**W**). Velocity profiles are developed with respect to elevation above ground (**z**) and radial distance (**r**) from the centre of the tornado. It is seen in the figure that the tangential velocity increases with radius up to a certain distance while the vertical profile quickly saturates with height. Radial velocity profiles have a peak at relatively low heights and then vanish. The vertical velocity wind profile is also of interest for OHL design as it counteracts the effects of the gravity loads induced by the conductors on the supports.

The wind flow of tornadoes can become complex, and all the different components can be expected to have large velocities at some point. As for a downburst, the direction and speed of the centre of the storm producing the tornado will affect the maximum horizontal wind speeds.

ASCE Manual 74 (2005) provides a simplified diagram of the regions of higher winds within a tornado (see **Figure 6**). As the rotary and translational components are combined, a zone of very high wind speeds develops in the right-hand side of the tornado for a counterclockwise wind field. It is important to note that the path width of the Fujita-

Pearson classification (in Table 1) is the estimated full width of the rotational component while the most destructive path is typically much less than one half of the full width.

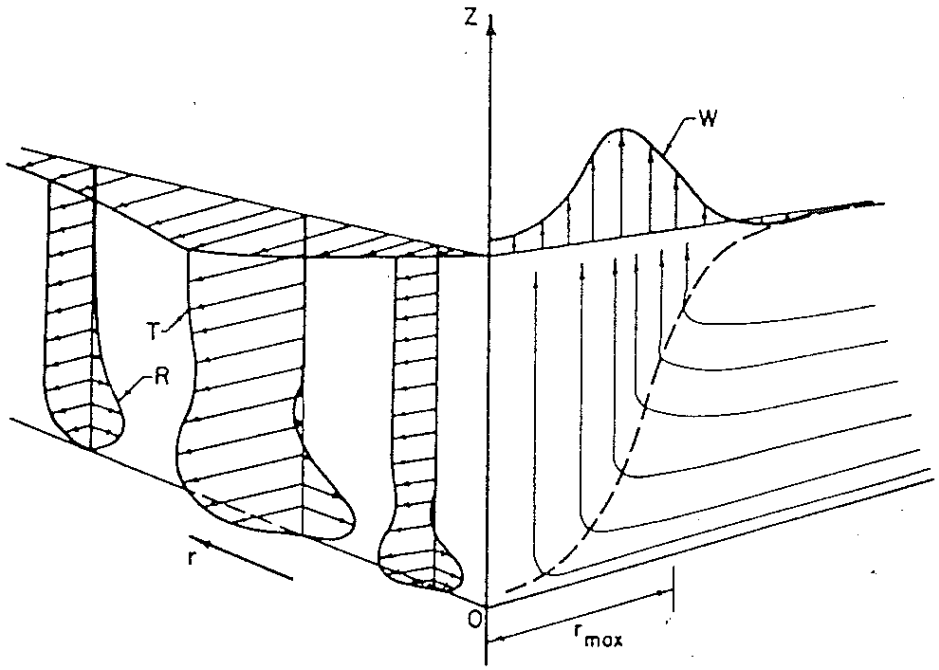

Figure 5 - Schematic wind field in a tornado vortex (Wen, 1975)

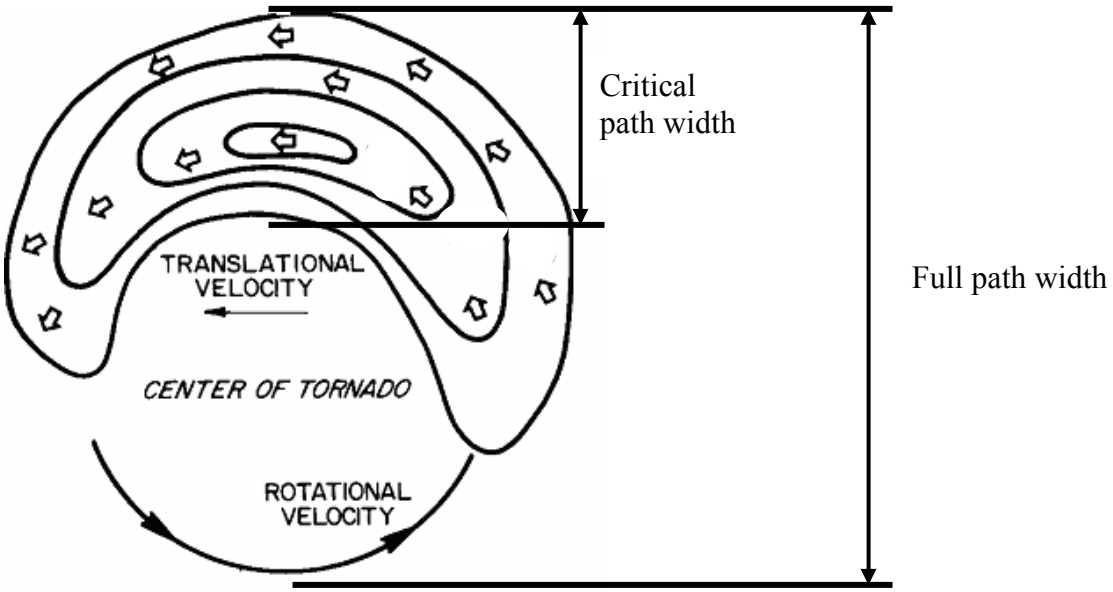

Figure 6 - Hypothetical pattern of tornado horizontal wind field (Adapted from ASCE, 2005)

More details regarding meteorological aspects of localized HIW events are available in CIGRÉ TB 256 (2004) and the reports of Langlois (2006 and 2007) contain an updated list of relevant references.

4. Risk assessment of localized HIW events

4.1 Challenges in recording events

When, where and how often do localized HIW occur? Those questions have proven to be difficult to answer. Most electric utilities – except in the United States and Argentina (for tornadoes), in Australia, Brazil, Argentina and South Africa (for downdrafts) – have no information available on local wind speeds in tornadoes and downdrafts. In the absence of sufficient information, it is impossible to develop a probabilistic model of these wind loads for overhead line design and only a deterministic approach may be adopted. Design values may be based on the "greatest credible event" for the area considered.

Many challenges are encountered when assessing the risk of these wind events, even when a data base of observations is available. Several factors affect the quality of data records:

- downdraft and tornado recording has a limited time span;
- it varies with the density of population – dense records do not necessarily correlate with the location of important lines;
- it is affected by the great physical complexity of these storms.

What makes overhead lines particularly vulnerable to localized HIW is the spatial extent of the system: the probability of a severe local wind event striking a line section is much higher than the probability of striking a single point.

4.1.1 Limited observation time span

The observation time span is an important factor for the development of reliable localized HIW risk models. Records are often limited to only a few decades of observations. For example, before the 1960s, the unknown phenomenon of downdraft would often go unreported, while some downdraft events would be reported as tornadoes. Changes in definitions and in the level of awareness of specialists and of the population in general led to a non-uniformity of records over time. It could also be argued that global climate changes make it extremely difficult to extrapolate the available historical data to have a rational basis for design loads.

4.1.2 Density of the observation mesh point and bias in densely populated areas

Another factor affecting the records is the density of population. This way, quality of records varies from one region to another. Since localized HIW, by definition, are small in extent, many events are not noticed when they occur in open space. Recording of wind speeds by anemometers, which is much more reliable than evaluations based on damages, is limited due to the possibility of measuring wind speed at a precise point only. Since the probability of a severe wind striking a point is very small, it would take many years of

data from an anemometer to predict with some accuracy the probability of that severe wind striking a line system of several hundreds of kilometers. Specialists generally rely on direct observation of the phenomenon to build databases. Hence, the probability of localized HIW is often underestimated in sparsely populated regions. However, even with a small data base, a confidence level may be provided considering the sample size and model error.

4.1.3 Physical complexity of localized HIW storms

A third challenge is the physical complexity of wind events. In fact, every severe storm event has a different wind field and therefore, the exact prediction of wind loadings is impossible. Wind speed and direction vary rapidly over time and the duration of the storm is difficult to predict. The only way to obtain useful data is to categorize wind events and to study common patterns in their wind field.

One last general problem lies in the interpretation of the categorization of localized HIW. It can be expected that a data set will tend to become overly standardized. For example, in the continental United States, where tornadoes are expected to occur often, there could be a bias towards identifying non-tornadic winds as tornadoes. The quality of data records in a region must be carefully verified before attempting any serious HIW risk assessment.

4.2 General risk modeling issues

For developing a proper risk model, an adequate probability distribution must be chosen which fits the observations available. Traditionally, the Type I Extreme-Value distribution (Gumbel distribution), is used to analyze annual extreme wind speeds. However, according to Holmes (1999), this distribution should not be used for winds originating from localized storms which occur as discrete events. The distribution proposed by Holmes is a Type III Extreme-Value which is more realistic when return periods need to be extrapolated beyond the data limits.

The question of the choice of distribution also points out the problem of dealing properly with extreme wind data in climates where different types of severe wind events occur. Twisdale (1982) argues that: “the most accurate prediction of wind-loading risk is obtained from a separate analysis of each wind-producing phenomena”. The fundamental issue is to statistically describe HIW as a distinct population of wind events: this is a first step towards the development of a probabilistic design philosophy for HIW.

Separate analysis of wind gusts from thunderstorms in the region of Sydney was performed by Gomes and Vickery (1976). They later developed a technique to analyze separately the wind speeds from different storm types and combine them into a single design wind speed (Gomes and Vickery, 1978). The importance of thunderstorm winds was demonstrated when Twisdale and Vickery (1992) showed that those winds dominated the records of many weather stations in the United States.

The distribution of localized HIW is not uniform over the planet. Nonetheless, failures due to HIW have occurred in various climates where they have hit structures which have not been designed for such loading conditions. In effect, most regions of the world should be concerned with the probability of HIW, while mitigation for those winds should be different from one climate to the other.

Several risk models have been developed for HIW and some of them are directly applied to overhead lines. Most of them consider only tornadoes, or only downdrafts. A brief review of the salient features of these models is provided in the following sections, while more details are presented in Langlois (2006).

4.3 Risk models for downdrafts

Downdraft risk modeling is a new area of research and is limited by the short period of data records. Only a few regions of the world, including the United States and Australia, have been studied for the probability of occurrence of downdrafts. During the NIMROD and JAWS projects in the United States, tens of microbursts were recorded, and statistical analyses were performed. In **Figure 7**, the yearly probability of occurrence (**P**) is plotted as a function of wind speed (**W**): it is seen that few observations are available for wind speeds above 30 m/s. Although the curves fit well on existing data, the extrapolation outside the range of the observations using the formulas provided is questionable.

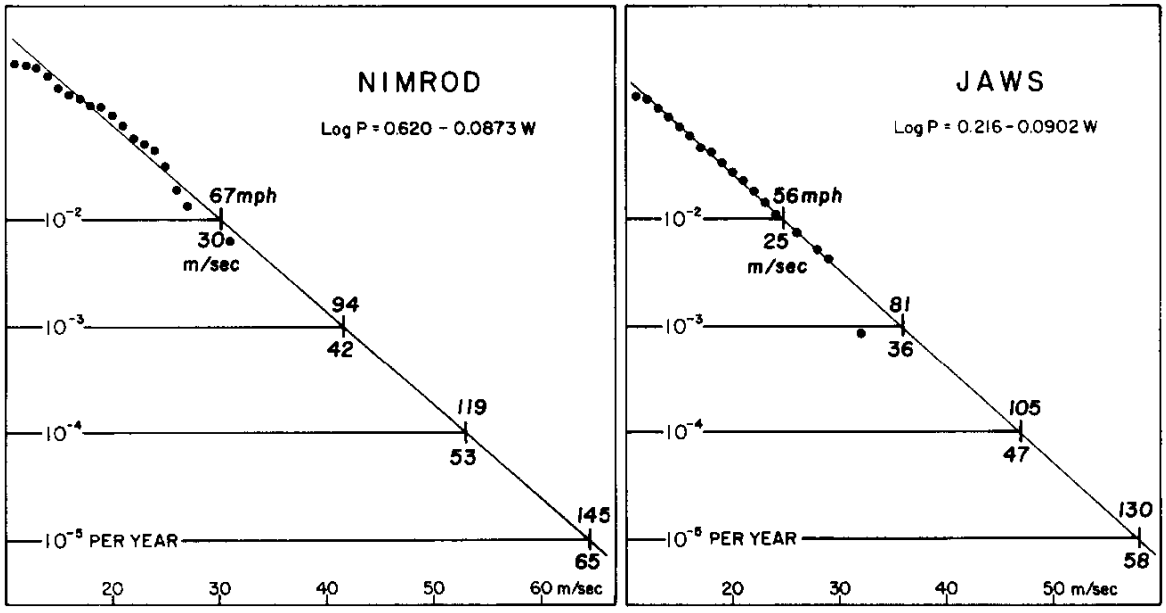

Figure 7 - Microburst wind speeds in the NIMROD and JAWS projects as functions of the occurrence probability per year (Fujita, 1990)

In Australia, downdrafts and their resulting damages are observed frequently. Holmes and Oliver (2000), based on a ESAA report, evaluated that for the state of New South Wales, the yearly average occurrence of downdrafts producing winds higher than 20.6 m/s at a

recording station is 2.0. The peak gust recorded for such events was 42.2 m/s. Similarly, in Queensland, the average is 2.35 per annum with a maximum recorded wind velocity of 51.5 m/s. Hawes and Dempsey (1993) added that for New South Wales, the frequency of microbursts is similar to that found during the NIMROD and JAWS projects and that a return period of around 100 years per hundred kilometers of overhead line is expected for a wind speed of 45 m/s.

Based on their observations of downdrafts, Australians have developed risk models for the intersection with transmission lines. A conceptual model is presented by Li and Holmes (1995) and Li (2000) which attempts a realistic simulation of wind loadings due to thunderstorms and accounts for the size effect of convective downdrafts. A less complex and well-accepted model is the one by Oliver, Moriarty, and Holmes (2000). From the following formula:

$$R_{V,L} = (\frac{w_v}{L}) * \left[\sum_{i=1}^{N} \Pr(v \geq V / |\sin(\theta_i - \varphi)|) * \Pr(\theta_i) * (|\sin(\theta_i - \varphi)|) \right], \quad \textbf{(Eq. 4.1)}$$

one can obtain the return period $\boldsymbol{R_{V,L}}$ of a downdraft event of average path width of $\boldsymbol{w_v}$ with wind speed $\boldsymbol{v}$ greater than threshold wind speed $\boldsymbol{V}$ crossing a line section of length $\boldsymbol{L}$. The average path width is assumed to be directly related to the threshold wind speed. The calculation relies on two probabilities (denoted by **Pr**(*event*) in the equation): the probability that the wind speed $\boldsymbol{v}$ exceeds the threshold wind speed $\boldsymbol{V}$ in direction $\boldsymbol{\theta_i}$ and the probability of the downdraft to occur in direction $\boldsymbol{\theta_i}$. The relative angle between the direction of the storm and the direction of the line is $\boldsymbol{\theta_i - \varphi}$, and the summation sign indicates that N downdraft occurrences in the various directions $\boldsymbol{\theta_i}$ are considered. In the formula, the length variable is in the denominator, which shows that the return period for damaging intersections decreases with the length of the line (Holmes, 2001).

An earlier version of this risk model is used by Letchford (1998) to study a line that had failed twice under HIW. Using the same model, Letchford and Hawes (2000) assessed the probability of failure of the entire high voltage transmission line network due to downdrafts in Queensland, Australia. The model generally predicts more failures due to downdrafts than what is really observed. This is due to both a conservative design process and a conservative extreme wind speed analysis.

Some other downdraft risk models were developed in other countries. For example, Schwarzkopf and Rosso (1982) developed the return period graph in **Figure 8** that is shown as an example in ASCE Manual 74 (ASCE 2005) – this risk model was proposed for the 4th 500 kV line project (650 km) in Argentina. It is noteworthy that a great merit of this graph is to indicate the variability of the model prediction with plots of confidence intervals, and to allow a direct comparison of tornado and downburst risks.

Downdraft risk models are quite similar to, and in fact originate from tornado risk models. However, downdrafts spatial impact is generally larger than that of tornadoes. Often, more than one span is enveloped by damaging winds and therefore, unlike for tornadoes, the wind loading on conductors is significant. For long lines not specifically

designed for localized HIW and perpendicular to the normal direction of thunderstorms, risk models usually yield very small return periods.

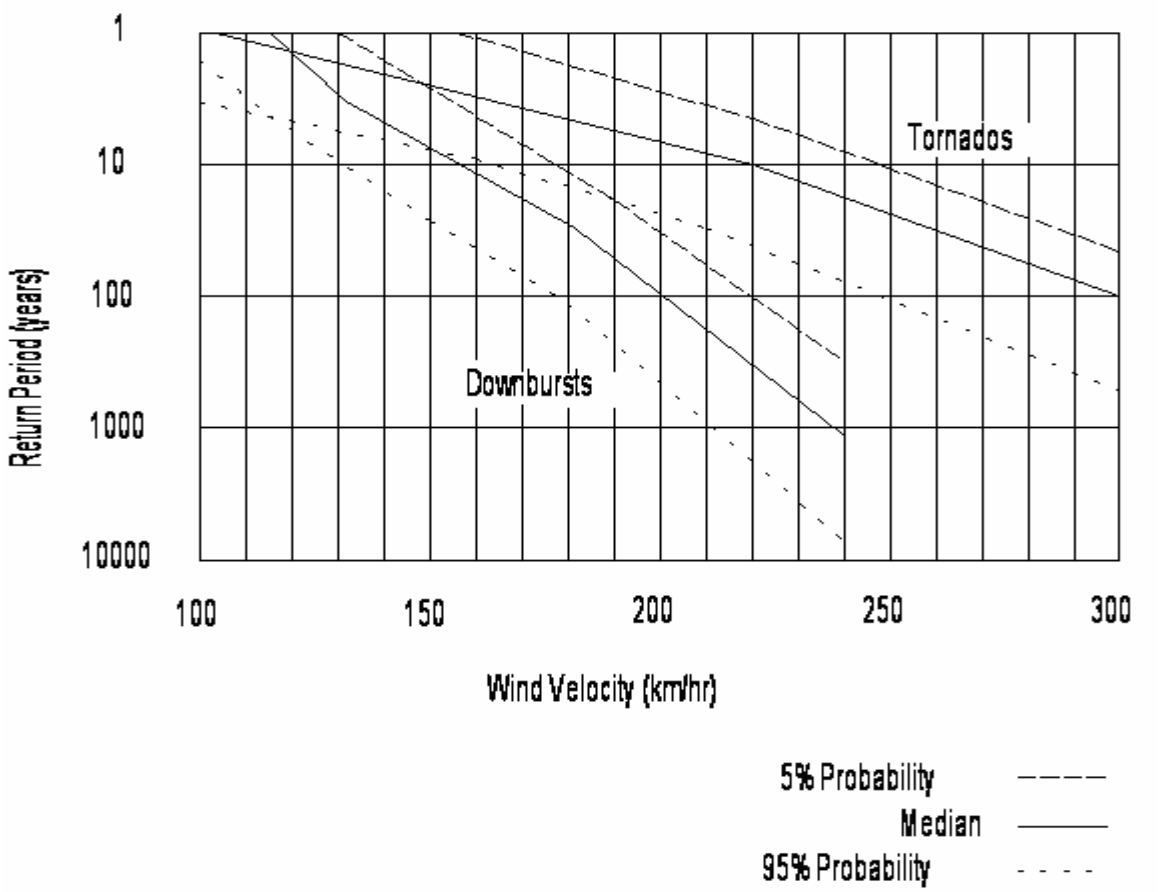

Figure 8 - Return period of wind speeds for downdrafts and tornadoes traversing a 650-km 500 kV line section in Argentina (ASCE, 2001)

4.4 Risk models for tornadoes

Most tornadoes, and more specifically those which do not cause structural damages, typically affect a width smaller than one line span (wind span). The focus of the tornado risk models is to consider wind on the line structures. This is based on the assumption that the probability of an entire span being loaded is small. Hence, risk assessment goes from looking at the probability of an event striking any point on a line, as for a downburst, to the probability of an event striking any support on a line. In general, tornadoes should cause damages less often than downbursts, but could possibly be more devastating due to higher wind speeds.

Tornado records are kept in most developed countries. The United States is by far the country where the largest number of tornadoes is reported with an average of 800 to 1000

each year for the contiguous states (ASCE, 1991). Recently the number of tornadoes was evaluated at 1200 per year for the whole country (Brooks *et al*., 2003), all severity levels combined. ASCE Manual 74 includes a map of the United States with the number of tornadoes recorded during a 30-year span for each one-degree squares of longitude and latitude. This map (not shown here) was developed by Tecson, Fujita, and Abbey (1979) and is also included in the ASCE Guidelines for Electrical Transmission Line Structural Loading (2005). In the ASCE 7 - Minimum Design Loads for Buildings and Other Structures (2002), another map (**Figure 9**) shows the extrapolation to a 100,000-year return period for the expected maximum tornadic wind speed in the continental USA. The three zones delimited on the map correspond roughly to the F1, F2 and F3 intensity tornadoes according to the original Fujita scale (**Table 1**).

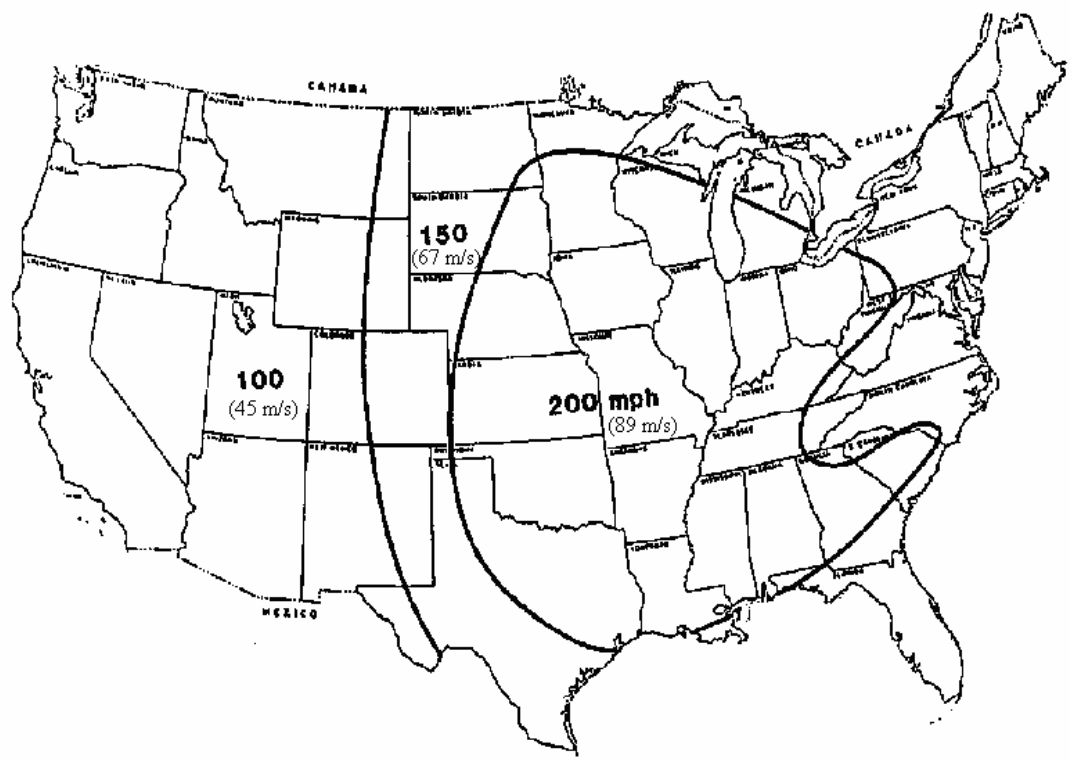

Figure 9 - Tornadic wind map of continental USA corresponding to a 100,000-year return period (ASCE, 2002)

Other authors have attempted to assess the frequency of tornadoes in South Africa (Milford and Goliger, 1994) and Argentina (Schwarzkopf and Rosso, 1982). Fujita (1973) was the first to review tornado activity around the world and similar work was done more recently by Goliger and Milford (1998). These studies identify the North American continent as being the area where most tornadoes occur. The Great Plains of the United States are, without any doubt, an area favorable to the formation of tornadoes. However, due to an increased awareness, a large portion of the tornadoes recorded are very small ones. Those small tornadoes were not reported a few decades ago, and in most parts of the world, are still not reported. Therefore, the difference between the frequency of events in the United States and elsewhere is probably smaller than what is shown in

the current records. For example, the recording efforts in Germany have increased the frequency from about 2 per decade before 1950, to 7 in the 1990s, to finally 20 in the year 2000 alone (Brooks *et al.*, 2003).

For the overhead distribution and transmission line industry, it is often more reliable to study risks looking directly at the number of HIW-related failures of lines in a region. The CIGRÉ Technical Brochure by Working Group B2.16 (2004) gives an idea of the frequency of line failures for some countries. In that same Technical Brochure, a useful world map of wind hazard is provided. It is mentioned that tornadoes of scale F2 and above will generally cause structural failure due to extreme turbulence and rotational wind structure.

The idea that all tornadoes produce extremely high and devastating winds and that nothing could be built to survive those events is no longer valid. Most records consider not only the number of tornadoes, but also their intensity. It is useful to know the percentage of low intensity tornadoes in a record because design criteria should be based on resisting most tornadoes and not necessarily the greatest possible tornadoes. This percentage certainly depends on the quality of the record, but for acceptable data, the number of F0 and F1 tornadoes is typically very high. For the Canadian Great Lakes region, the percentage of tornadoes less than F2 is about 80 % (*Notes on meeting*, 1993). For the United States, the ASCE Manual 74 (2005) suggests that 86 % of recorded tornadoes are F2 or smaller.

5. Effects of localized HIW on OHL

5.1 Current knowledge

The knowledge on the effects of localized HIW on overhead lines is limited. Research on the wind field and on the risk assessment - see Langlois (2006) for an overview - of those events has shown that their effects are very different from the conventional boundary layer wind effects.

In general, the wind loading due to tornadoes or downdrafts could take various forms depending on the regional characteristics. Therefore, the most realistic prediction for those wind loads is that they could be anything other than the synoptic wind load usually accounted for in design codes. Nonetheless, there are still ways to simplify the effects of localized HIW and to economically reduce the impact of those winds on structures.

Based on observations of wind damages on overhead lines, Carpena and Finzi (1964) proposed an early design philosophy specifically for tornado wind loads. Their view was that a support should be able to resist a number of different directional tornado loadings, rather than only one very high transverse loading based on synoptic wind data. It is suggested to adopt a similar design philosophy for all localized HIW effects on overhead lines. A description of these effects as they are understood today follows, which provides the rationale for the specific design guidelines provided in Section 7 of this Technical Brochure.

The effects of localized HIW on OHL structures depend on whether the dominant pressure loads are transferred from the conductors to the support or directly applied to the support. The load path of the conductor loads is designed to flow through the primary structural system: from the conductor attachment point, through the supporting cross arm, beam or earth wire peak and then through the main legs and bracing members (for self-supporting lattice towers) or through the mast and guying system (for guyed structures). In a typical synoptic wind loading acting transversely to the line, the wind distributed to the structure through the conductors, represents a large part of the total horizontal load on the supports. The position of the resultant transverse load is then very high on the support, near the geometric center of the conductors. This applies in general to most line supports such as poles and tubular or lattice H-frames.

It is relevant to discuss the particularities of the localized HIW load paths in classical lattice towers with inclined main legs. By design, the intersection of the main leg slopes (see **Figure 11 a**) is usually selected to coincide nearly with the horizontal resultant of the synoptic wind load on tower and conductors in order to minimize the stresses in the bracing members between the main tower legs. As the wind load on tower panels below the bracing members does not affect those bracing members, very high towers are divided in several parts with different slope, separated by waists.

If the vertical profile of the wind load on the tower is constant or shows a peak at low altitude, such as in the case of convective downdrafts, the resultant wind load will be lowered, so that the internal force in the bracing members will increase. If the wind load on the conductors is not considered, such as in the case of tornadoes, the resultant wind load will be lowered significantly so that all bracing members could be overstressed.

This suggests that one way of increasing the reliability of existing classical lattice towers with inclined legs against failures due to localized HIW would be to increase the strength of their bracing members. A special loading scenario is suggested in Section 7 to account for these cases where the wind-on-tower loads may govern the design of tower bracings.

5.2 Effects of downdrafts

A simplified downdraft loading is found in some works (Langlois, 2006), but there is no consensus yet on this matter.

Downdrafts are known to have a larger impact than tornadoes in relation to their spatial extent, i.e. more than one span can be affected by an event. However, the wind speed at any point is highly dependent on its elevation and location with respect to the center of the storm, while the maximum wind speed is more related to the formation height of the storm cell. Also, downdraft wind loading varies greatly depending on the development stage at the moment the structure is hit. If a downdraft is close to touch down, high downward vertical winds are expected, but after touch down, the load is mainly horizontal (Savory *et al*., 2001), with possibly some upward vertical load due to the formation of a ring vortex. Hence, from a design loading perspective, horizontal effects are the most significant.

Based on wind tunnel simulations, Letchford and Hawes (2000) argue that since a typical downdraft can create HIW up to a height larger than 150 m, it can be assumed that supports are fully loaded over their total height with some gradation in the ground line zone. It is fair to say that to have the maximum impact on a support, a downdraft would be wide enough to engulf both spans either side of it, such that the wind loads on the conductors transferred to the support are those of the full wind span. However, even narrower downdrafts of the order of one span can also have significant effects. There is evidence that, unlike synoptic winds, these narrow wind fronts are well correlated horizontally such that span reduction factors should not be used. For instance, a convective downdraft of 800 m diameter would reach a height of about 30 to 40 m, which is within the support height in most single-circuit lines.

A worst-case design scenario should consider that the conductors of a few consecutive spans could be fully loaded. This is always the case for distribution lines or low voltage sub-transmission lines where spans less than 200 m are common.

Some authors have suggested that no span reduction factors should be used for a downdraft loading case (Oliver et al., 2000) compared to synoptic wind. This idea is based on observations of very well-correlated high gusts over a large area during

downdrafts. Dempsey and White (1996) have suggested that a patch-wind load acting only on the top sections of the support and conductors would represent the high wind shears expected during downdrafts. The most elaborate downdraft loading model available to date is found in the Australian ENA C(b): 2006 and is summarized in Section 6.1.

5.3 Effects of tornadoes

A number of sources have expressed the characteristics of a simplified tornado wind loading for OHL design. Many of them are articles illustrating design practices used by some utilities, or recommendations formulated by the overhead distribution and transmission line industry. The most important ones are summarized in Section 6. One common point to these simplified loadings is that the wind load on conductors is neglected due to the assumed very narrow path of a tornado.

In the event of a tornado directly hitting a support, the wind load on conductors may be small compared to the load on the structure itself. As discussed in Section 5.1, the centre of wind loading is therefore lowered and significant forces develop in bracing members; if buckling of one of those bracings occurs, the tower may fail in a shearing mode. This failure mechanism is often observed for structures suffering a very narrow HIW storm such as a tornado (Dempsey and White, 1996). For guyed structures, the complex wind loading patterns on guy wires and lattice sections may have various effects because of geometric non linearity (large deflections). Global lateral displacements and local bending of structure sections under direct wind may result in significant eccentric axial compression in the mast (P-δ effects) that further increases the bending moments in the masts. Also, the wind profile can influence the shear distribution in the masts of guyed-Y and Delta-guyed structures (Ishac & White, 1995).

5.4 Numerical simulations

Along with the observation of line failures, the development of numerical models for wind loading and line structures is a valuable mean to evaluate the effects of HIW. From models of simulated wind fields of a downdraft or a tornado, it is feasible to compute wind loads to be used in finite element analysis of supports and line sections. This approach was used successfully by Savory *et al*. (2001) for a lattice transmission tower subjected to both a tornado and a small microburst severe loading. Their model was limited to one tower and the conductor loads were neglected, thus representing a much localized HIW event. As expected, the tornado loading created a shear failure but the local microburst affected the tower moderately.

In another study, Hoxey *et al.* (2003) simulated the response of both a self-supporting lattice structure and a guyed structure to a downdraft. In this case, wind on conductors was also included and the guyed structure was, generally, more affected than the self-supporting tower. The failure mode simulated was a rupture of the cross arm of the primary member above the guy fixings. More recently, Shehata *et al.* (2005) have simulated downdraft quasi-static loading on a guyed structure based on a CFD wind field

model by Hangan (2002). Although these analyses still need refinement to explain actual line failures, they can give a good indication of the distribution of forces in any specific structure due to a variety of localized HIW loading scenarios.

Chay and his collaborators (Chay and Albermani, 2005 & Chay *et al*. 2007) have also conducted numerical simulations with a focus on the dynamic aspects of tower response. In their first paper, simulations on single-degree-of-freedom systems indicated that adding comparable gusts of wind on a translating downburst wind profile and on a boundary layer wind profile generated more dynamic response in the latter case. This is explained by the fact that structures are affected by the high intensity downbursts for a much shorter duration than comparable synoptic winds. Their more recent work analysed a realistic guyed tower in simulated downburst winds. The results indicate only a small dynamic amplification of the response (of the order of 5%) when the turbulent component of the downburst loading was accounted for compared to the quasi-static loading model.

5.5 Topographic effects

Local topographic effects have been studied extensively in boundary layer wind tunnels and these studies have led to the introduction of wind speed-up factors in design based on synoptic winds. A few physical simulations of downdrafts, including one by Letchford and Illidge (1999), have shown that speed-up factors for localized HIW are smaller than for boundary layer winds. It should be noted that this observation was based on stationary jet models and could be different for storms with high translational velocities. These effects need further study, as suggested by CIGRÉ Technical Brochure 256 (2004).

5.6 Dynamic effects

Thunderstorm winds usually change very rapidly with time, but the possible existence of dynamic amplification effects in overhead line structures due to localized HIW has only been investigated very recently at the University of Queensland in Australia, in relation with downburst loadings on guyed masts. (Chai *et al*. 2006 & 2007)

For reasonably short supports and line spans, the dynamic response is expected to be small (Holmes, 2001). Also, for high wind speeds, Matheson and Holmes (1981) have suggested that dynamic response is not dominant due to the development of high aerodynamic damping that would limit any resonance that could occur in conductors due to natural frequencies below 1 Hz and relatively close to wind forcing frequencies. Classical lattice towers (with the exception of very tall towers used in river crossings) generally have higher natural frequencies and are rarely affected by the dynamic properties of wind (if we exclude possible fatigue). However, it is not excluded that some guyed structures could be affected especially if some guy wires become slack during the storm, due to sudden changes in wind intensity and/or direction. Cross-rope suspension structures may also be sensitive to dynamic fluctuations in cross-rope tensions induced by the HIW wind loads.

The small number of complete time history records available makes it difficult to assess the dominant frequencies of localized HIW events. Also, except for the recent work of Chay and his collaborators that was reviewed above, the wind field models used in numerical simulations usually do not address local turbulence effects which may or may not be present.

It is clear that for downbursts to have a significant dynamic effect on overhead line supports, the frequency content of the turbulent wind component must match that of the structures (conductor/tower system) subjected to the wind loads. At present, limited knowledge on turbulence in downbursts and the small number of numerical case studies published to date are insufficient to support design guidelines to account for dynamic effects of downbursts on overhead lines.

5.7 Damages due to projectiles

It is recognized that flying debris generated by localized HIW wind storms pose a serious threat to overhead lines, especially for distribution lines. It is not possible to quantify the probability of failure associated to debris and projectiles in a built environment, although strict maintenance management of surrounding vegetation may contribute to reduce it. Such failures are considered as accidental and are best addressed in global design considerations for line security. This Technical Brochure therefore considers the direct effects of wind pressures on the overhead line.

Projectiles during tornadoes can lead to major damage if they hit objects in their way. Projectiles may also be an issue in convective downdrafts where most building structures and vegetation that are stripped are within 10 m of the ground and they are blown horizontally. These projectiles, typically projected structural debris and objects in the path of the storm, or found in nature, such as trees, shrubs or twigs, are abundant and it is rare that any tornado event will not contain projectiles. There are many anecdotic and photographic accounts of the effects of tornado-generated projectiles that can do a lot of damage to structures, including overhead lines. This issue is all the more important in urban or semi-urban environments and distribution lines are especially prone to projectile-induced damage.

It is clear that some overhead line failures due to projectiles are unavoidable, even if the tower structure is reinforced to resist extreme wind pressures. This emphasizes the need to ensure that a support failure does not propagate in a cascade and the importance of a reconstruction strategy that allows for fast repairs.

5.8 Transverse cascades

A major concern in the overhead line industry is the avoidance of line cascades. Most line cascades are longitudinal when triggered by the failure of a structural element that

maintains tension in the conductors. Transverse cascades of overhead lines are almost exclusively initiated by HIW and large synoptic wind storms. When a support falls in the transverse direction, its adjacent effective spans become longer and large conductor tensions are induced at the adjacent structures, creating significant transverse and longitudinal load imbalances. If these supports also fail, the collapse may progress, forming a transverse cascade. Transverse cascading was often in the past mistakenly perceived as "multiple failures caused by a *wall of wind* overcoming all the fallen structures" (ASCE, 2001). However, during major wind storms such as tropical cyclones, hurricanes, typhoons and extra-tropical storms it is possible that multiple failures of a line do occur due to the potential initiation of multiple closely-spaced gusts, thus increasing the likelihood of triggering cascading effects.

Prevention of cascades by effective failure containment measures is a critical aspect of line design and is an effective way of minimizing the potential damages due to HIW.

The issue of line cascades triggered by a line component failure during a localized HIW storm is beyond the scope of this Technical Brochure but will be addressed in the broader context of overhead line security in future work of CIGRÉ SC B2. CIGRÉ Technical Brochure No. 174 on "Load Control Devices on Overhead Transmission Lines" (2000) issued on behalf of WG 22.06, and the WG B2.06 report "Generic Specification for an Ideal Load Control Device" (2007) accessible on the SC B2 website deal with devices developed to limit the damage to overhead lines after a possible support failure.

6. Overview of localized HIW-resistant design provisions

6.1 ENA C(b)1-2006, Australia

ENA (2006) specifies a design procedure for microburst loading that is very similar to that for synoptic wind loading. Australia is divided into 11 regions of microburst activity and a microburst design wind speed varying with the desired line reliability level is assigned for each region. All design wind speeds are based on a line length of 100 km (line reliability is assumed inversely proportional to its length) and a microburst gust width of 500 m. To give an indication of their range, the design wind speeds vary from 46 m/s to 60 m/s for a return period of 100 years. Wind forces are considered both on the supports and the conductors and span reduction factors must be not less than 0.9 for spans less than 500 m. The wind speed is further multiplied by a microburst wind direction factor that depends on the region considered and on the critical wind direction (perpendicular to the line).

This document is currently being reviewed: the draft document should be published late 2007 for public comment and will be incorporated into an Australian / New Zealand design standard. It will provide a slightly different but for more defined downdraft wind regions as well as synoptic wind regions; their respective span reduction factors, velocities and related loadings. Tornado wind loadings for F2 events are provided and will be only a requirement for major inter regional lines.

It appears that the prescriptions of ENA C(b)1-2006 are not strictly applied by the present line designers and all new transmission lines designed recently in HIW-prone areas have incorporated additional and more specific HIW criteria. The ENA guidelines have been successfully applied by a distribution company in New South Wales. One practice that has been applied is to provide a patch loading load case with downdraft wind applied to the conductors and to the upper portion of the target support above 15 m. This partial loading on the tower is based on the observed damages on towers for several downburst failure events, to account for the development of shift in high wind shears above ground. Such shifting wind shears have been shown to depend on the surface boundary layer roughness and terrain features by wind tunnel work performed by Lechford and Illidge (1999).

6.2 ASCE Manual 74

ASCE Manual 74 (1991) and its draft revision (ASCE, 2005) provide many useful information on localized HIW, especially on tornadoes. The approach for tornado-resistant design is to consider a uniform wind loading corresponding to a moderate tornado scale (F1 or F2) applied only to the transmission structure over the full structure height from any direction, as in the ENA standards. It is further suggested to remove the

effect of the conductor dead load as the vertical wind component in a tornado can possibly lift the conductors. The design recommendations for downdraft loading vary with the size of the event. For a small microburst, it is suggested to use the same load as for the tornado.

The 2005 draft revision of ASCE Manual 74 also introduces an interesting discussion on transverse cascades and the corresponding failure modes observed on supports.

6.3 Hidronor (currently Transener), Argentina

Hidronor was the first utility to report the use of a special tornado loading in OHL design for its Alicura 500 kV line (Behncke and White, 1984). It recognized that although OHL supports were not likely to resist a direct hit by very severe tornadoes, it was feasible to mitigate the effects of F2 tornadoes with maximum wind speeds up to 220-240 km/h (60-67 m/s). Static analysis was carried out on V-guyed structures subjected to a uniform wind loading based on those speeds and coming from any direction. The tornado loading required only minor reinforcement to a few members near the top and the bottom of the masts. In this project, earth wire peak fuses were also used to mitigate potential transverse cascades.

6.4 Eskom, South Africa

While Hidronor's justification for a tornado-resistant design load was found in past line failures (namely on its 500 kV El Chocon line), Eskom tried to evaluate the actual risk that represent tornado winds for transmission lines based on tornado risk models and event records. The design criteria and their assumptions are documented in Behncke *et al*. (1994). The tornado loading chosen is more conservative than the one recommended by the ASCE (1991), with an F2 tornado wind of 250 km/h (70 m/s) applied to the tower only, while considering the dead weight of conductors. This simplified model was based on the recommendations of a previous review (CSIR, 1992) of tornado loading models. Behncke *et al*. (1994) insisted that tornado loads are especially critical on guyed structures such as V-guyed and cross-rope structures.

6.5 Hydro One, Canada

Ishac and White (1995) have developed the tornado-resistant design criteria used by Hydro One in Ontario, Canada. Their tornado stochastic load model is based on a very high proportion (92%) of small intensity tornadoes (F2 or less) recorded in the region studied. The tornado wind speed applied to a line segment is proportional to its boundary layer extreme wind speed equivalent. It is much higher than normal extreme values, but is applied to the tower only. For example, the highest tornado wind speed used is 67 m/s (240 km/h, intensity F2) for regions where the extreme synoptic design wind speed is 44.4 m/s (160 km/h).

6.6 CIGRÉ Technical Brochure 256 (2004)

Although the main focus of the CIGRÉ Technical Brochure 256 (2004) was to describe the characteristics of all major types of HIW storms and tropical cyclones as well, it made recommendations in relation to the spatial effects of wind gust types.

For regions prone to tornadoes, it recommends that line supports should be designed to resist a uniform F2 tornado wind speed coming from any direction and a rotational wind with no loads on the conductors.

For downdraft, it recommends the full uniform wind from any direction be applied on both the structures and the supported conductors. It further suggests including the effects of surface roughness on the wind approach to the line, as they tend to introduce high wind shears above ground. Therefore it is also recommended that no wind be considered below 15 m. CIGRE Technical Brochure 256 also recommends that wind span reduction factors should be ignored for downdrafts.

7. Proposed simplified loading cases for localized HIW

7.1 General

It is generally accepted by OHL line designers that extreme synoptic wind data provide an acceptable basis for geometric line support design (also based on electrical clearances) and for loading cases where wind is of secondary importance compared to icing or other conditions. For tropical cyclones, typhoons and hurricanes, there is no consensus yet on the best approach apart from recommending as in Australian Standard AS/NZS 1170.2-Wind Actions, the use of the synoptic wind method with increased wind velocities. However, such a wind field model is not representative of the wind loads induced by localized HIW storms on overhead lines. This is why Working Group B2.06 is proposing the simplified loading cases listed in Section 7.3 for downdrafts and tornadoes. These loading cases are intended to cover critical wind load paths in the support that would differ from those obtained with conventional synoptic wind loading.

The approach suggested by the Working Group B2.06 is to consider HIW loading cases that are localized: they do not apply to several consecutive spans of a line section but rather focus on a specific support of the line section, designated as the target support. The general idea is adapted from Behncke and White (2006) who advocate direct consideration of HIW (for example the 3-s gust used in ASCE Manual 74) without correction for height (the velocity profile is taken as uniform), gust effect (this effect is already included in the choice of the wind speed for the HIW), span length (the target structure is assumed fully loaded by its wind span), terrain roughness and topography. This is a simplified approach that has been adapted to include some consideration of spatial effects as shown in Table 5 with partial tower loading affecting horizontal load paths in the towers. As for the effects of terrain roughness and topography, they may be considered where they are known to be significant.

On the schematic plan view of a line section in **Figure 10**, the target tower is the central one and a single-circuit AC line configuration is shown in a horizontal configuration. Only two equal spans (with span length **S**) are shown for simplicity. It is assumed that the target tower is in suspension although most considerations are also applicable to strain structures where conductor tension loads are present. In practice, earth wires can be assumed anchored to the tower. In the figure, the storm of front dimension **w** hits the line transversely. As a result, the tower is subjected to a horizontal transverse load (resultant $\mathbf{Q_t}$) and the supported conductors are subjected to a uniform horizontal load of $\mathbf{Q_c}$. Other incident wind directions **φ** will reduce conductor loads and, for most tower types, increase wind loads on the tower. For $\boldsymbol{\varphi \neq 0°}$, $\mathbf{Q_c}$ and $\mathbf{Q_t}$ are conveniently represented by their longitudinal and transverse components, where the effect of the longitudinal component of $\mathbf{Q_c}$ may be ignored if the sag is small compared to the wind span.

When the two adjacent spans are fully loaded, (**w = 2S**), the portion of conductor wind load $\mathbf{Q_c}$ actually transferred to the target tower is calculated based on the full wind span **S,** that is 50% of **w**. However, when the adjacent spans are only partially loaded (**w < 2S**), the target tower will collect most of the load. A simple static rule can be established to calculate the effective width of conductor load to be transferred to the tower as a fraction of **w** equal to **1- 0.25(w/S)** (Behncke and White, 2006).

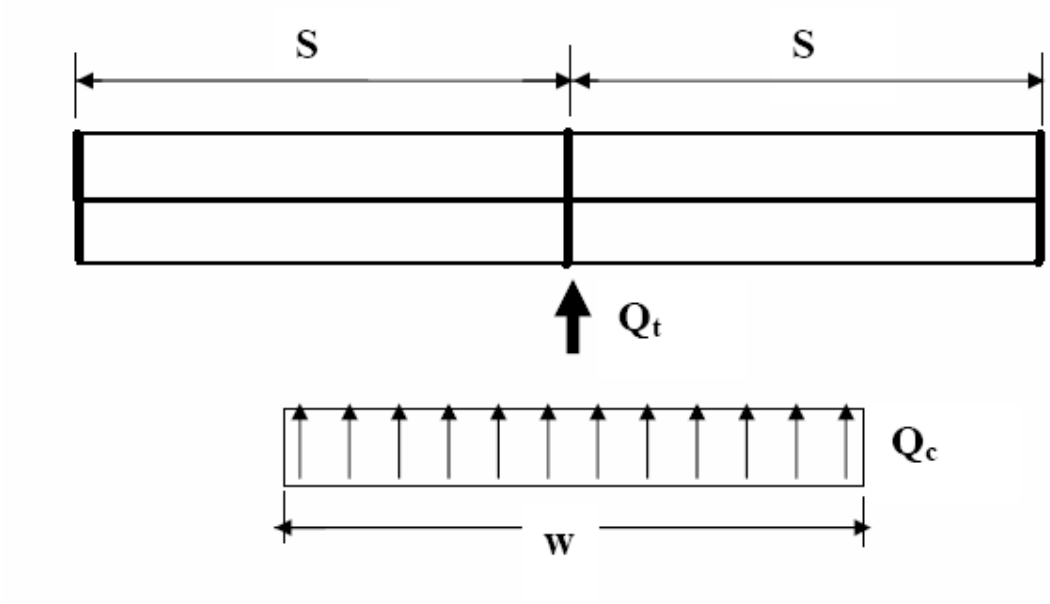

Figure 10 - Plan view of a line section subjected to localized HIW

Table 4 defines the nomenclature of the main design variables used in the descriptions of the simplified loading cases presented in Section 7.3. Some of the geometric variables are shown on **Figures 10** and **11. Figure 11** illustrates two schematic tower geometries for the localized HIW load cases: a classical self-supporting lattice tower and a guyed structure. Adaptation to other support geometries and line configurations is readily feasible.

Table 4 - Nomenclature for the proposed localized HIW loads	
$\mathbf{h_c}$	Height above ground of the conductor attachment point
$\mathbf{h_i}$	Height above ground delimiting a partial wind loading on a support (Figure 11)
$\mathbf{q_c}$	Uniform wind pressure on a conductor
$\mathbf{q_f}$	Uniform wind pressure on a windward tower face (in lattice towers)
$\mathbf{q_t}$	Uniform wind pressure on a tower and its ancillary Components
$\mathbf{Q_t}$	Horizontal resultant of the wind-on-tower load
$\mathbf{Q_c}$	Horizontal wind-on-conductor load
S	Span length
w	Path width of the localized HIW storm
φ	Angle of incidence of the storm front with respect to the transverse direction

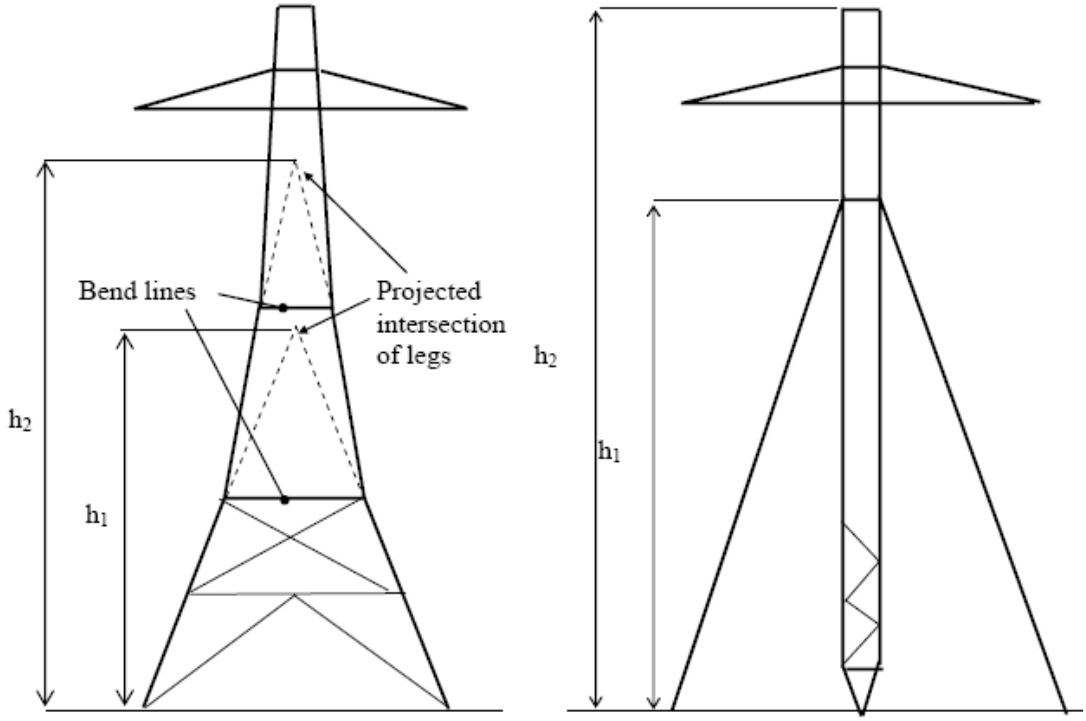

a) Self-supporting tower **b) Guyed structure**

Figure 11 - Schematic support geometries for localized HIW loading cases

7.2 Selection of wind pressures and storm widths

Where sufficient local information on wind speeds in downdrafts and tornadoes is available, reliability-based values of q_c, q_t and q_f with the required return period may be calculated. Where insufficient data is available, a deterministic "greatest credible value" may be used for the area, or alternatively a value predicted to achieve the lowest lifetime cost for the overhead line may be used.

In the absence of any more specific information on tornado hazard, CIGRÉ TB 256 (2004) provides valuable information on the characteristics of wind storm phenomena. It is suggested here to use a uniform pressure (constant with height) corresponding to the maximum threshold of an F2 tornado – a wind speed of 70 m/s and a storm path width **w** = 160 m. Note that the damaging width would be a fraction of this value (cf. **Figure 6**). However, this has little influence in this Technical Brochure since wind-on-conductor loads are not included in the tornado loading case proposed in Section 7.3. This wind speed lies in the range of the EF3 tornado (**Table 2**) and correlates well with observed damages to overhead line supports in the United States (**Table 3**). As indicated in **Table 1**, this design level would likely encompass about 85% of the tornadoes occurring in the United States.

The 70 m/s wind speed also corresponds to the upper limit of downdraft winds ever recorded or experienced. It can be argued that it is too severe and unrealistic to consider

such a large deterministic value in an area where no reliable observations are available. For a downdraft, the selection of a reasonable maximum wind speed is paramount since the path width is assumed to cover the entire two spans (i.e. **w = 2S** in **Figure 10**). So the conductor wind load $\mathbf{Q_c}$ transferred to the tower is calculated based on the full wind span.

The wind pressures used in the calculations represent the effects of localized HIW storms on the target structure. They are determined from a uniform wind velocity profile without correction for height, gust effect, span length, terrain roughness and topography. Wind pressures $\mathbf{q_t}$ and $\mathbf{q_f}$ shall incorporate a drag coefficient appropriate to the tower body. For lattice towers, it is common practice to use a drag coefficient based on the tower solidity ratio. Wind pressure $\mathbf{q_c}$ shall also incorporate a drag coefficient appropriate to the type of conductor.

For calculation of conductor tension, where appropriate, still air conditions may be assumed and the temperature shall be taken as the mean of the temperature range within which the HIW events are expected to occur. No atmospheric icing is considered.

7.3 Simplified loading cases

7.3.1 Loading cases for localized HIW

In regions where localized HIW events now appear to be more frequent than previously anticipated, utilities are looking at simple ways of reducing the risk of catastrophic failures. In this context, Working Group B2.06 recommends the six simplified loading cases summarized in **Table 5.** These loading cases are meant to provide a conservative estimate of the response of the target support to downdrafts and tornadoes, with particular consideration of the wind load paths in the support. Except for the partial support loading (cases DPB and DPA) for downdrafts, which is specific to lattice towers with inclined legs and guyed supports, all the proposed loading cases are applicable to all types of line supports.

As indicated in the last column of the table, several of these loading cases have already been developed or used (as is or with modifications) by some utilities on specific projects or are currently part of some design standards or recommended guidelines. For these utilities, the proposed loading cases in Table 5 are not new and may not be deemed sufficient. In this context, Working Group B2.06 recommends that these loading cases be considered as minimum requirements.

	Table 5 - Design loading cases for localized HIW				
	HIW load case	Horizontal wind direction	Wind on conductor	Wind on support	Also developed or used by
Downdraft	DT	Transverse	yes	Full height – all types of supports	ENA Australia
	DL	Longitudinal			
	DO	Oblique			
	DPB	Transverse and longitudinal	no	Below h_i for lattice tower (i = 1, 2, …)	Exclusive to CIGRÉ (Figure 5 a & b)
				Below h_1 for guyed structure	
	DPA	Transverse and longitudinal	yes	Above h_1 for guyed structure	ENA Australia
Tornado	T(φ)	Multidirectional: φ = 0°, 45°, 90°	none	Full height – all types of supports	Eskom South Africa
					Hidronor (Transener) Argentina
					ASCE Manual 74 & HydroOne Canada (weightless conductors)

7.3.2 Simplified loading cases for downdrafts

- **DT: Full transverse wind on conductors (w = 2S) and support**

Loading case DT should yield the worst condition for the transverse shear forces at the tower base. No vertical wind pressure is applied and the dead load of the conductors is included, as well as the effects of conductor tension if applicable.

- **DL: Full longitudinal wind on the support only**

Loading case DL will create the worst longitudinal shear forces at the tower base and will be critical for some bracing members in the longitudinal faces.

- **DO: Full oblique wind on conductors and tower**

The most critical direction for the oblique loading case DO will depend on:

- the ratio of the transverse and longitudinal areas of the tower;
- the fraction of the wind load on the conductors $\mathbf{Q_c}$ versus the wind load directly applied on the tower $\mathbf{Q_t}$.

For lattice supports, it is suggested to consider at least the most critical case (typically **φ = 15º** to **20º**) for the main leg members and the reactions on lattice tower foundations. More directions can be investigated, especially **φ = 30°, 45º** if the oblique loading proves

critical. No vertical wind pressure is applied and the dead load of the conductors is included.

- **DP: Partial transverse and longitudinal wind on the support**

It is suggested that, because overhead line supports are normally designed for wind loadings applied over the entire support and on the conductors, they may be vulnerable to localized HIW loading applied to part of the support only.

Loading case DPB addresses the problem of shear failures in the lower parts of lattice self-supporting towers with sloping legs, that is failure of transverse and longitudinal bracings rather than main leg members. Its purpose is to identify potential weaknesses in the transverse and longitudinal direction. It is understood that loading case DT will be more critical for most other members and for reactions on the foundations.

Referring to **Figure 11 a** for a lattice tower, it may be noted that the centroid of the total wind loading assumed for design often approximately coincides with the intersection point of the legs (at elevation $\mathbf{h_1}$ or $\mathbf{h_2}$, or in this interval), which means that very small axial forces will be predicted in the bracing members for the panel below. However, if similar wind loadings are applied to part of the tower only, with low or reversed wind loading on the remainder, the same bracing members will experience much larger loads. The values $\mathbf{h_1}$ or $\mathbf{h_2}$ are chosen to give the most severe condition, for a given wind intensity, for the bracing members located in the lower and intermediate parts of the tower, respectively. A uniform wind pressure $\mathbf{q_t}$ shall be assumed to act on the tower and upon any ancillaries attached to it from ground level to height $\mathbf{h_1}$. The same will also be considered if a second bend-line is present from ground to $\mathbf{h_2}$. If more bend-lines are present further heights $\mathbf{h_3}$, $\mathbf{h_4}$, etc., shall be defined similarly and additional load cases shall be considered if the point of intersection of the legs is below the top of the tower.

For a guyed structure (**Figure 11 b**) the highest bending in the mast at height $\mathbf{h_1/2}$ is likely to occur with wind loading applied over $\mathbf{h_1}$ only.

Loading case DPA represents conductor loads and loads directly applied on the top portion of guyed towers (above $\mathbf{h_1}$**)**. It represents the effects of high wind shears that can occur in any horizontal direction.

7.3.3 Loading case for tornadoes

- **T(φ) Multi-directional wind on support only**

In most self-supporting lattice towers, several wind directions are investigated to find the most critical effects for all tower members. Uplift winds are not considered on the supporting structure. The self-weight and the tension loads of the conductors are included.

For guyed structures, it is suggested to consider the both cases where the self-weight and conductor tension loads are included and excluded. Large in-span mast deflections introduce important axial load eccentricities that may significantly reduce the overall stability of the support.

Technical Brochure 256 recommends designing towers withstanding the high swirling/rotational wind of F2 tornadoes on the structure only. If the rotational wind is also applied to the conductors at the left and at the right of the tower with an opposite transverse wind load, the total transverse wind load on the conductors is zero, so that the wind load on the support only is justified.

7.3.4 Special considerations for members in windward faces

For classical lattice towers subjected to localized HIW storms, special consideration shall be given to members in the windward faces that are directly subjected to large pressures. In particular, all bracings in the windward faces shall be capable of resisting, simultaneously with any axial force calculated form the loading cases in **Table 5**, the bending moments generated by the wind pressure $\mathbf{q_f}$ acting on the bracings and any other members or ancillaries attached to them. Similarly, plan and hip bracings shall be capable of resisting the loadings passed into them by the action of wind on the tower face. Note that for this calculation the proportion of the wind loading applied to the windward face of the tower shall be considered only. Wind pressure $\mathbf{q_f}$ shall incorporate a drag coefficient appropriate to the tower face but is considered constant with height.

7.4 Transverse cascades

In addition to the consideration of localized HIW loads on supports detailed in Section 7.3, a simple static design check against transverse cascading is recommended, as a special security load case. In fact, this load case could represent any transverse failure of a support in the bare conductor condition. As suggested in the 2005 draft version of ASCE Manual 74, it should be based on the calculation of residual static forces at conductor attachment points on adjacent supports due to a transversely fallen suspension support. The general approach is to consider the important reduction in conductor slack in a span adjacent to a fallen support.

We stress again that the important issue of transverse cascading is beyond the scope of this Technical Brochure but will be addressed in the broader context of overhead line security in future work of CIGRÉ SC B2.

8. Important limitations and research needs

In many regions of the world not exposed to atmospheric icing, localized High Intensity Winds pose the greatest risk to failure of overhead lines. Some utilities operating in these regions have already put in place codified procedures that provide a level of mitigation of the effects and provide increased security of overhead lines. For these utilities, the proposed loading cases in Table 5 are not new and may not be deemed sufficient.

In other regions where localized HIW events now appear to be more frequent than previously anticipated, utilities are looking at simple ways of reducing the risk of catastrophic failures. In this context, the simplified loading cases recommended in Section 7 are meant to account only for localized HIW effects on a target support. Their simplifying assumptions will require further validation through numerical simulations and/or physical observations. An example of such validation is provided in Appendix A to this Technical Brochure. It presents excerpts from a numerical study by Langlois (2007) who tested a total of 28 loading cases including 22 simplified HIW loading scenarios on four self-supporting lattice towers and compared the analysis results to those of traditional synoptic wind loadings. It should be noted that the four examples are all towers that were not originally designed to resist HIW effects. The analysis models assume that the tower members respond linearly and elastically to the applied loads. It is understood that this assumption is no longer valid under extreme loads. However, the results of the study are used for comparison purposes only – post-elastic analysis is outside the scope of this work – and this is why member usage (calculated axial load/member elastic capacity) exceeds 100% in some cases.

In direct relation to the loading cases suggested in Section 7, Langlois has verified that:

a) The assumption of a simplified uniform wind speed with height is conservative.

b) The maximum tower member forces do not typically occur when the tornado or downdraft hits in the transverse or longitudinal directions, but at some angle in between depending on the drag area of each face. The critical wind direction for a given member mostly depends on its position in the tower. This is also true for the synoptic wind on the suspension tower. In general:
   - The internal forces in the transversal bracing members are maximum for $\varphi \approx 0°$.
   - The internal forces in the longitudinal bracing members are maximum for $\varphi \approx 90°$;
   - The internal forces in the leg members are maximum for $\varphi \approx 0°$ for synoptic winds and convective downdrafts, but in oblique direction $\varphi \approx 45°$ for tornadoes, where the wind load on conductors is not considered (See **Appendix C**).

c) Partial wind loading on towers (without wind load on conductors), especially below the intersection point of the tower legs, may be critical for some horizontal and panel bracings.

d) Partial wind loading on towers above the intersection point of the tower legs or above 15 m was not found clearly conclusive in the cases studied. More simulations with due consideration of the backflow pressures on the conductors are necessary before reasonable simplified loading cases can be proposed.

e) Tornado loads (without wind on conductors) govern mostly the bracing members in the bottom part of the towers.

f) The proposed transverse downdraft load (denoted as DT in **Table 5**) is nearly equivalent to a severe transverse synoptic wind load case in terms of the distribution of member forces for the load cases studied.

g) Particular bracing design using the tension-only assumption may become problematic when non-conventional HIW loadings are considered. Slender members with very low buckling strength may never recover their original configuration and capacity when panels respond in the inelastic range.

Other relevant observations and conclusions are presented in the **Appendix A**. It is hoped that more studies will be generated by industry to test more hypotheses for a variety of towers. In particular, studies on guyed structure response are lacking.

At present, the suggested loading cases seem to fit observations and current design practice for tornadoes and convective downdrafts. However, more research is needed to study the interaction of localized winds with supports. Recent developments in computational fluid dynamics and in finite element analysis of fluid/structure interactive models provide a great opportunity to improve our understanding of the effects of many sources of HIW on lines.

More research and development is also needed on the important topic of risk assessment of overhead lines under localized HIW. We acknowledge that there is significant variability and uncertainty in the meteorological parameters and in the actual loads transferred to the line supports. These uncertainties are compounded by the linear configuration and spatial extent of overhead lines. Stochastic analysis and risk assessment are essential tools to quantify the benefits of HIW-resistant line design.

9. Conclusions

In many regions of the world not exposed to atmospheric icing, localized High Intensity Winds pose the greatest risk to failure of overhead lines. However, only a few countries have put in place codified procedures that provide a level of mitigation of the effects and provide increased security of overhead lines.

Some other countries, as presented in **Section 6**, have adopted mitigation measures only for specific projects. It should be emphasized that the effectiveness of these measures has not been proven. Such a proof is indeed very difficult to obtain unless a reinforced line section fails under conditions that are directly related to an HIW storm.

In other regions where localized HIW events now appear to be more frequent than previously anticipated, utilities are looking at simple ways of reducing the risk of catastrophic failures.

The goal is not to over design OHL supports so as to reduce to a minimum any probability of failure. However, the reliability of supports to localized HIW storms can be increased significantly with relatively simple improvements to the design loading assumptions as applicable for the particular HIW region.

For existing lines on classical supports designed using boundary layer wind profiles, it is feasible to increase significantly the survival of supports to localized High Intensity Wind storms with relatively simple improvements to the lateral and transverse resistance of the structures such as higher diagonal bracing capacity in self-supporting towers and higher flexural mast rigidity in guyed structures. For new supports, appropriate design loadings applicable to the predominant wind storm type of the region will necessarily influence the detailed design.

Six simplified design loading cases are proposed in this technical Brochure to account for the effects of localized High Intensity Winds on overhead line supports, with special considerations of downburst load paths for classical sloped leg self-supporting lattice towers and guyed supports. They are also generally applicable to any type of line support. Working Group B2.06 recommends that these loading cases be considered as minimum requirements for HIW-resistant design overhead lines, recognizing that those utilities with more detailed codified procedures in place are already complying with these requirements.

Clearly, design of new lines can easily integrate the proposed design load cases for localized HIW. However, extensive and costly mitigation on existing supports may be more difficult to justify considering the many uncertainties and limited knowledge on the effects of localized HIW storms on lines. When the hazard is real and its mitigation impractical, security measures can be implemented to reduce the probability of cascading

failures following the collapse of a support and to ensure rapid recovery of power delivery. This issue is beyond the scope of this Technical Brochure but will be addressed in the broader context of overhead line security in future work of CIGRÉ Study Committee B2.

10. References

American Society of Civil Engineers (ASCE). (1991). *Guidelines for electrical transmission line structural loading* (ASCE Manual No. 74). New York.

American Society of Civil Engineers (ASCE) (2002). *Minimum design loads for buildings and other structures* (ASCE Manual No. 7). Reston, VA.

American Society of Civil Engineers (ASCE) (2005). *Guidelines for electrical transmission line structural loading, draft revision* 2005 (ASCE Manual No. 74). New York.

Battan, L. J. (1984). *Fundamentals of meteorology*. Englewood Cliffs, NJ: Prentice-Hall.

Behncke, R. H., and White, H. B. (1984). Alicura 500 kV transmission system. *Proceedings of the International Conference on Large High Voltage Electric Systems (CIGRÉ)*, *22-02*, Paris, France.

Behncke, R. H. and White, H.B. (2006). Applying Gust Loading to Your Lines. *Proceedings of the 9th International Conference on Overhead Lines - Design, Construction, Inspection & Maintenance*, 27-30 March, Fort Collins, Colorado, USA, 151-155.

Behncke, R. H., White, H. B., and Milford, R. V. (1994). High intensity wind and relative reliability based loads for transmission line design. *Proceedings of the International Conference on Large High Voltage Electric Systems (CIGRÉ)*, *22-205*, Paris, France.

Brooks, H., Doswell, C., III, Dowell, D., Holle, R., Johns, B., and Jorgenson, D. (2003). Severe thunderstorms and tornadoes. In T. D. Potter & B. R. Colman (Eds.), *Handbook of weather, climate, and water: Dynamics, climate, physical meteorology, weather systems, and measurements* (pp. 575-619). New York: John Wiley & Sons.

Carpena, A., and Finzi, M. (1964). Wind damage on transmission lines. *Proceedings of the International Conference on Large High Voltage Electric Systems (CIGRÉ)*, *229*, Paris, France.

Chay, M.T., and Albermani, F. (2004). A review of downburst wind models for dynamic analysis of lattice structures, *Developments in mechanics of structures and materials – Proceedings of the 18th Australian conference on the mechanics of structures and materials*, vol. 1, 353-358.

Chay, M.T., and Albermani, F. (2005). Dynamic response of a SDOF system subjected to simulated downburst winds, *Proceedings of the Sixth Asia-Pacific Conference on Wind Engineering*, 12-14 September, Seoul, South Korea.

Chay, M.T., Albermani, A., and Wilson, R.J. (2006). Numerical and analytical simulation of downburst for investigating dynamic response of structures in the time domain, *Engineering Structures*, 28(2), 240-254.

Chay, M.T., Wilson, R.J. and Albermani, A. (2006). Gust Occurrence in Simulated Non-stationary Winds, *Fourth International Symposium on Computational Wind Engineering,* 16-19 July 16-19,Yokohama, Japan.

Chay, M.T., Albermani, F., and Wilson, R.J. (2007). Response of a guyed transmission line tower in simulated downburst winds. *12th International Conference on Wind Engineering*, Cairns, July 2007, 5p.

CIGRÉ SC 22 WG 06 (2000). *Load control devices of overhead transmission lines* (CIGRÉ Technical Brochure No. 174), International Council on Large Electric Networks, Paris.

CIGRÉ SC 22 WG 06 (2001). *Probabilistic Design of overhead transmission lines on current practices regarding frequencies and magnitude of high intensity winds* (CIGRÉ Technical Brochure No. 178), International Council on Large Electric Networks, Paris.

CIGRÉ SC B2 WG 16 (2004). *Report on current practices regarding frequencies and magnitude of high intensity winds* (CIGRÉ Technical Brochure No. 256), International Council on Large Electric Networks, Paris.

CIGRÉ SC B2 WG 06 (2006). *Reliability based design methods for overhead lines - Advantages, applications and comparisons* (CIGRÉ Technical Brochure No. 289), International Council on Large Electric Networks, Paris.

CIGRÉ SC B2 WG 06 (2008). *Big Storm Events - What we have Learned* (CIGRÉ Technical Brochure to be published in 2008), International Council on Large Electric Networks, Paris.

Council for Scientific and Industrial Research (CSIR). (1992). *Transmission line loading due to narrow winds* (No. 550 23121). Johannesburg, South Africa: Eskom.

Davenport, A. G. (1995). How can we simplify and generalize wind loads? *Journal of Wind Engineering and Industrial Aerodynamics, 54/55*, 657-669.

Dempsey, D., and White, H. B. (1996). Wind wreak havoc on lines: The cause of most transmission structure outages in many areas of the world is high intensity wind. *Transmission and Distribution World*, 32-42.

Energy Networks Association (2006). *Guidelines for design and maintenance of overhead distribution and transmission lines* (ENA C(b)1-2006).

Fujita, T. T. (1971). Proposed characterization of tornadoes ad hurricanes by area and intensity. Satellite and Mesometeorology Research Report 91, the University of Chicago, Illinois, USA, 42 pp.

Fujita, T. T. and Pearson, A.D. (1972). Results of FPP Classification of 1971 and 1972 Tornadoes. *Eighth Conference on Severe Local Storms*, American Meteorological Society, Boston, MA, 142-145.

Fujita, T. T. (1973). Tornadoes around the world. *Weather wise, 26*, 56-62 & 78-83.

Fujita, T. T. (1981). Tornadoes and downbursts in the context of generalized planetary scales. *Journal of the Atmospheric Sciences, 38*(8), 1511-1534.

Fujita, T. T. (1990). Downbursts: Meteorological features and wind field characteristics. *Journal of Wind Engineering and Industrial Aerodynamics, 36*(Part 1), 75-86.

Goliger, A. M., and Milford, R. V. (1998). Review of worldwide occurrence of tornadoes *Journal of Wind Engineering and Industrial Aerodynamics, 74-76*, 111-121.

Gomes, L., and Vickery, B. J. (1976). On thunderstorm wind gusts in Australia. *Australian Civil Engineering Transactions, CE18*(2), 33-39.

Gomes, L., and Vickery, B. J. (1978). Extreme wind speeds in mixed wind climates. *Journal of Industrial Aerodynamics, 2*(4), 331-344.

Hangan, H. (2002). Numerical simulations of high intensity winds. Downburst simulations. Retrieved January 5, 2006, from http://www.iclr.org/pdf/Hangan report downburst simulations.pdf

Hawes, H., and Dempsey, D. (1993). *Review of recent Australian transmission line failures due to high intensity winds.* Paper presented at the April meeting of the Task Force on High Intensity Winds on Transmission Lines, Buenos Aires, Argentina.

Hjelmfelt, M. R. (1988). Structure and life cycle of microburst outflows observed in Colorado. *Journal of Applied Meteorology, 27*, 900-927.

Holmes, J. D. (1999). Modeling of extreme thunderstorm winds for wind loading of structures and risk assessment. *Proceedings of the 10th International Conference on Wind Engineering*, Copenhagen, Denmark.

Holmes, J. D. (2001). *Wind loading of structures*. New York: Spon Press.

Holmes, J. D., and Oliver, S. E. (2000). Empirical model of a downburst. *Engineering Structures, 22*(9), 1167-1172.

Hoxey, R., Robertson, A., Toy, N., Parke, G. A. R., and Disney, P. (2003). Design of an experimental arrangement to study the wind loads on transmission towers due to downbursts. *Advances in Fluid Mechanics, Fluid Structure Interaction II, 36*, 395-404.

International Electrotechnical Commission (IEC) (1991). *Loading and strength of overhead transmission lines*, Technical Report 826, Technical Committee 11, 2nd Ed., ISO, Geneva, Switzerland.

International Electrotechnical Commission (IEC) (2003). *Design criteria of Overhead Transmission Lines*, International Standard 60826, Technical Committee 11, 2nd Ed., ISO, Geneva, Switzerland.

Ishac, M. F., and White, H. B. (1995). Effect of tornado loads on transmission lines. *IEEE Transactions on Power Delivery, 10*(1), 445-451.

Langlois, S. (2006). *Effect of high intensity winds on overhead transmission lines*. McGill University, Department of Civil Engineering and Applied Mechanics. Structural Engineering Series Report no. 2006-02, 68 p. http://digital.library.mcgill.ca/pse/docs/CER_pdfs/Structural/CER_no_06-2.pdf

Langlois, S. (2007). *Design of Overhead Transmission Lines Subject to Localized High Intensity Wind,* M.Eng. Thesis, Department of Civil Engineering and Applied Mechanics, McGill University, Montréal, Canada.

Letchford, C. W. (1998). *Wind environment experienced by Tarong-Mt England transmission line at Harlin during the thunderstorm on 18 March 1998* (No. 10764). Powerlink.

Letchford, C. W., and Hawes, H. (2000). Risk assessment to improve reliability of transmission facilities exposed to sub-tropical high wind storm events. *Proceedings of the International Conference on Large High Voltage Electric Systems (CIGRÉ)*, *22-104*, Paris, France.

Letchford, C. W., and Illidge, G. (1999). Turbulence and topographic effects in simulated thunderstorm downdrafts by wind tunnel jet. *Proceedings of the 10th International Conference on Wind Engineering*, Copenhagen, Denmark.

Letchford, C. W., Mans, C., and Chay, M. T. (2002). Thunderstorms - Their importance in wind engineering (a case for the next generation wind tunnel). *Journal of Wind Engineering and Industrial Aerodynamics, 90*(12-15), 1415-1433.

Li, C. Q. (2000). Stochastic model of severe thunderstorms for transmission line design. *Probabilistic Engineering Mechanics, 15*(4), 359-364.

Li, C. Q., and Holmes, J. D. (1995). Failure prediction of transmission line structural systems under severe thunderstorms. *Australian Civil Engineering Transactions, CE37*(4), 309-314.

Lin, W.E, Novacco, C. and Savory, E. (2006). Transient simulation of a microburst outflow: Review and proposed new approach. *Proceedings of Canadian Society of Mechanical Engineers (CSME) Forum 2006,* Kananaskis, Alberta, May (CD-ROM)

Lin, W.E. and Savory, E. (2006). Large-scale quasi-steady modelling of a downburst outflow using a slot jet. *Wind and Structures, 9, 419-440.*

Lutgens, F.K., and Tarbuck, E.J. (2001). The atmosphere: An introduction to meteorology (8th ed.). Upper Saddle River, NJ, Prentice Hall.

Mason, M. S., Letchford, C. W., and James, D. L. (2005). Pulsed wall jet simulation of a stationary thunderstorm downburst, Part A: Physical structure and flow field characterization. *Journal of Wind Engineering and Industrial Aerodynamics, 93*(7), 557-580.

Matheson, M. J., and Holmes, J. D. (1981). Simulation of the dynamic response of transmission lines in strong winds. *Engineering Structures, 3*(2), 105-110.

McCarthy, P., and Melsness, M. (1996). *Severe weather elements associated with September 5, 1996 hydro tower failures near Grosse Isle, Manitoba, Canada* (No.). Winnipeg, Manitoba, Canada: Manitoba Environmental Services Centre - Environment Canada.

McDonald, J.R., and Mehta, K.C. (2006). A recommendation for an Enhanced Fujita Scale (EF-Scale). Technical Report submitted to The National Weather Service. Wind Science and Engineering Center, Texas Tech University, Texas, USA. http://www.wind.ttu.edu/EFScale.pdf

Milford, R. V., and Goliger, A. M. (1994). Tornado activity in South Africa. *Journal of the South African Institution of Civil Engineers, 36*(1), 17-23.

Milford, R. V., and Goliger, A. M. (1997). Tornado risk model for transmission line design [Electronic version]. *Journal of Wind Engineering and Industrial Aerodynamics, 72*(1-3), 469-478.

Nolasco, J. F. (1996). Analysis of recent transmission line failures. In CIGRÉ WG 22.06 (Ed.), *Review of IEC 826: Loading and strength of overhead lines* (pp. 87-98). Paris.

Notes on meeting. (1993). Paper presented at the April meeting of the Task Force on High Intensity Winds on Transmission Lines, Buenos Aires, Argentina.

Oliver, S. E., Moriarty, W. W., and Holmes, J. D. (2000). Risk model for design of transmission line systems against thunderstorm downburst winds. *Engineering Structures, 22*(9), 1173-1179.

Peabody, A. B. (2004). *Applying shock damping to the problem of transmission line cascades*. Ph.D. Thesis, Department of Civil Engineering and Applied Mechanics, McGill University, Montréal, Canada.

Peyrot, A. H., Kluge, R. O., and Lee, J. W. (1978). *Longitudinal loading tests on a transmission line* (EPRI EL-905). Palo Alto, CA: Electric Power Research Institute.

PLS-CADD (Version 7.62+). (2006). Madison, WI: Power Line Systems.

Savory, E., Parke, G. A. R., Zeinoddini, M., Toy, N., and Disney, P. (2001). Modelling of tornado and microburst-induced wind loading and failure of a lattice transmission tower. *Engineering Structures, 23*(4), 365-375.

Selvam, R. P., and Holmes, J. D. (1992). Numerical simulation of thunderstorm downdrafts. *Journal of Wind Engineering and Industrial Aerodynamics, 44*(1-3), 2817-2825.

Shehata, A. Y. (2006) *Analysis and Behaviour of Guyed Transmission Line Structures Under Downburst Wind Loading. Ph.D. Thesis.* Department of Civil and Environmental Engineering. The University of Western Ontario, London, Canada, 174 p.

Shehata, A. Y., El Damatty, A. A., and Savory, E. (2005). Finite element modeling of transmission line under downburst wind loading. *Finite Elements in Analysis and Design, 42*(1), 71-89.

Schwarzkopf, M. L. A., and Rosso, L. C. (1982). Severe storms and tornadoes in Argentina. *Proceedings of the Conference on Severe Local Storms*, San Antonio, TX.

Tecson, J. J., Fujita, T. T., and Abbey, R. F., Jr. (1979, October). Statistics of U.S. tornadoes based on the DAPPLE tornado tape. *Proceedings of the 11th Conference on Severe Local Storms*, Kansas City, MO.

TOWER (Version 7.61). (2006). Madison, WI: Power Line Systems.

Twisdale, L. A. (1982). Wind-loading underestimate in transmission line design. *Transmission & Distribution, 34*(13), 40-46.

Twisdale, L. A., and Vickery, P. J. (1992). Research on thunderstorm wind design parameters. *Journal of Wind Engineering and Industrial Aerodynamics, 41*(1-3), 545-556.

Wen, Y.-K. (1975). Dynamic tornadic wind loads on tall buildings. *ASCE Journal of the Structural Division, 101*(ST1), 169-185.

Wen, Y.-K., and Chu, S.-L. (1973). Tornado risks and design wind speed. *ASCE Journal of the Structural Division, 99*(ST12), 2409-2421.

Wood, G. S., Kwok, K. C. S., Motteram, N. A., and Fletcher, D. F. (2001). Physical and numerical modelling of thunderstorm downbursts [Electronic version]. *Journal of Wind Engineering and Industrial Aerodynamics, 89*(6), 535-552.

Appendices

Appendix A presents a summary of a report by Langlois (2007) who tested several localized HIW loading cases on four self-supporting lattice towers. Results are compared with the basic loading case using the synoptic wind loading method of the International Standard IEC 60826. The most relevant excerpts are given below.

Appendix B gives the equations and input parameters for the numerical wind models of Wood *et al*. (2001) for the downdrafts and Wen (1975) for the tornadoes.

As the information about the design data and the strength analysis of the lattice towers is confidential, the loading cases and the internal compression forces in the tower members are not given. Only relative values of compression forces compared with the basic load case are mentioned. The results of a more theoretical approach that is only valid for tangent self-supporting towers with statically determinate braced panels are summarized in **Appendix C**.

A. Case studies of localized HIW and comparison with synoptic wind loading

A.1 Numerical modeling of overhead lines

A.1.1 Modeling of the towers

Several simulations were performed to evaluate the effects of various High Intensity Wind (HIW) load cases on four self-supporting lattice towers. All simulations are static linear analyses. Only two-span line sections needed to be modelled. For the target tower frame-truss models were used. Load cases are chosen to match previous suggestions found in the literature concerning HIW effects and in this Technical Brochure (TB). Internal axial forces in tower members were compared for the various load cases. It is of interest to identify which load cases are critical to the type of tower examined and which groups of members receive relatively higher forces under those load cases.

Table A.1 provides a summary of the properties of each analyzed tower.

Table A.1 - Properties of lattice towers examined for HIW load cases

Tower name	Peabody	Wisconsin	Canadian Bridge 0°	Canadian Bridge 15°
Short name	PB	WI	CB0	CB15
Source	Peabody (2004)	Peabody (2004)	Hydro-Québec	Hydro-Québec
Tower type	Tangent	Tangent	Tangent	Angle (15°)
Insulator type	Suspension I	Suspension I	Suspension V	Dead-end
Tower height	28.5 m	28.0 m	49.5 m	39.1 m
Height h_1	22.0 m	24.0 m	> 49.5 m	34.3 m
Wind span	350 m	350 m	450 m	450 m
Conductors	Cardinal 54/7 ACSR	Ibis 26/7 ACSR	Bersimis 42/7 ACSR	Bersimis 42/7 ACSR
Outside diameter	30.4 mm	19.9 mm	35.1 mm	35.1 mm
Ultimate tension	150 kN	72.5 kN	154 kN	154 kN
Max. conductor temperature	75 °C	75 °C	75 °C	75 °C
Number of sub-conductors	1	1	4	4
Circuit	Single	Double	Single	Single
Configuration	Horizontal	Vertical	Horizontal	Horizontal
Voltage level	230 kV	138 kV	735 kV	735 kV

The geometry and steel angle shape properties were modeled in TOWER (2006). Frame-truss models were used. Beam elements were used wherever the model needed stability in the rotational degrees of freedom. For calculating wind loads, each tower was divided into sections usually representing one tower panel. To match common practice of designers, most redundant (or secondary) members (that reduce the buckling length of primary members) were not included in the models. In order to account for the presence of these members in the calculations, additional vertical dead load and equivalent drag areas were added manually.

A.1.2 Peabody Tower

This single-circuit suspension tower was designed by Alan B. Peabody for the purpose of his Ph.D. work at McGill University (Peabody, 2004). The structure was meant to support a 230 kV line (see **Figure A.1**). Unlike the other three towers, this is only a prototype structure and it has never been built. The objective of the design process for this structure was to provide realistic tower stiffness in the analysis of anti-cascading damping devices. The tower configuration is a typical horizontal single-circuit.

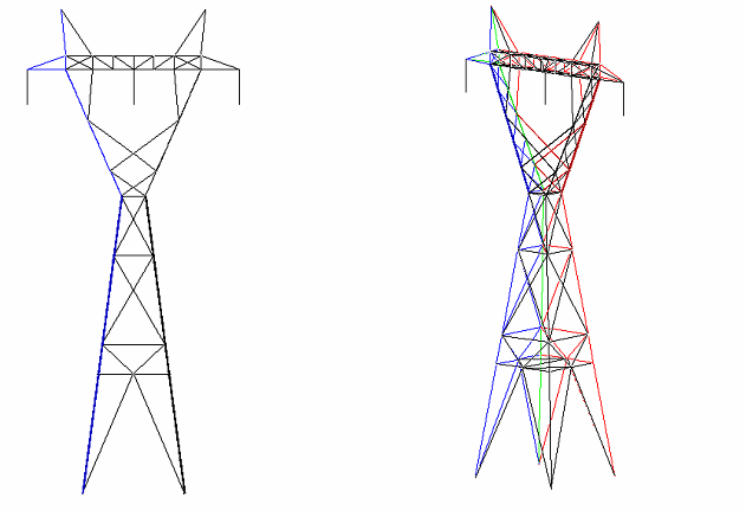

Figure A.1 - Peabody tower model

A.1.3 Wisconsin Tower

The second tower originates from a 138 kV line owned by Wisconsin Power and Light. Destructive tests were performed on this line section by the Electric Power Research Institute (EPRI). This is a classical double-circuit suspension tower (see **Figure A.2**).

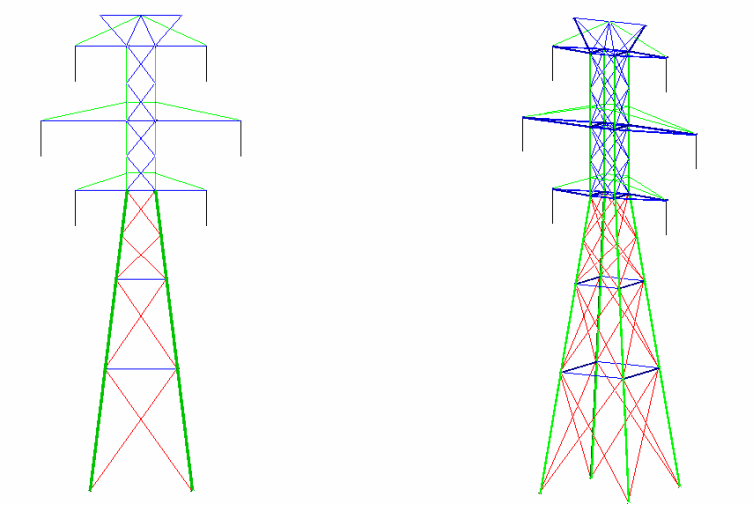

Figure A.2 - Wisconsin tower details (Peabody, 2004)

A.1.4 Canadian Bridge 0° and 15° Towers

Structural details of these two towers were obtained from Hydro-Québec. The towers were designed in 1963 and reinforcement was recently added. These single-circuit lattice towers are used on 735 kV lines in the Churchill-Manicouagan-Montreal corridor. Angles 0° and 15° refer to the horizontal line orientation change they can accommodate. The first tower is a suspension structure (**Figure A.3**) and the second an angle structure (**Figure A.4**).

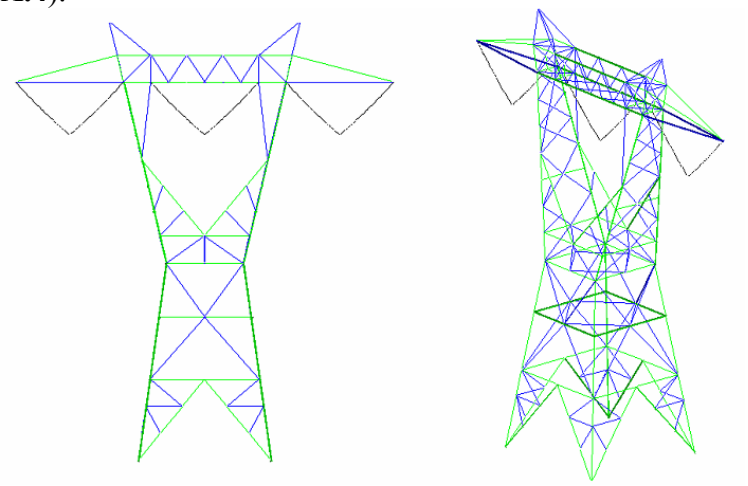

Figure A.3 - Canadian Bridge 0° suspension tower model

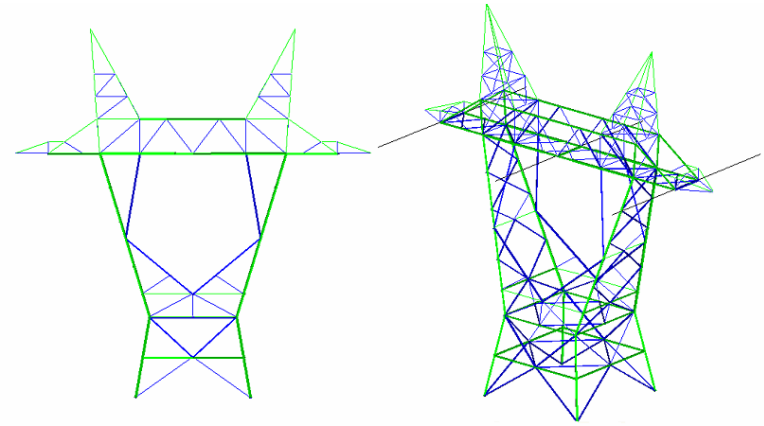

Figure A.4 - Canadian Bridge 15° angle tower model

The other main difference between the two towers is their respective height. The suspension tower is higher by 10 m due to the inclusion in the model of a leg extension. The models are slightly different in the area of the tower truss to comply with their respective insulator types: the suspension tower requires more frame elements in this section to support the V strings.

A.2 Description of load cases

A.2.1 Wind calculation models

Two wind calculation models available in PLS-CADD were considered: the IEC 60826 (2003) model, which is based on the international IEC standard, and the "wind on all" model.

For the "wind on all" calculation model, the wind speed is not adjusted with height and the gust response factor is equal to 1. The exposed area of the tower is calculated from the vertically projected surface of all the members defined in the tower section on a plane perpendicular to the wind direction. It is therefore assumed that no shielding effect occurs between parallel faces. The TOWER manual (2006) suggests using an overall drag coefficient of 1.6 for that model.

A.2.2 Comparison of wind loading models

Table A.2 shows a comparison of the two models for the Peabody tower. The "wind on all" model was tested at various wind speeds. No adjustment is made with height and no gust response factor is used for conductors. The conductor wind loads are therefore much lower than those calculated with the IEC 60826 method. In fact, as shown in the table, the total load on conductors is almost equivalent for a wind speed of 30 m/s in the IEC method and a wind speed of 45 m/s in the other method. For the structure loads, a wind speed of 30 m/s in the IEC method is equivalent to a wind speed of about 35 m/s for the "wind on all" model.

Table A.2 – Comparison between wind load models for the Peabody tower						
Method	Drag factor		Wind speed	Loading		
	Conductors	Tower		Conductors	Tower	Total
	-	-	m/s	%	%	%
IEC 60826	IEC	IEC	30	56	44	100
Wind on all	1	1.6	30	27	31	58
			35	36	42	79
			40	48	55	103
			45	60	70	131

A.2.3 Load cases

The load cases tested on the self-supporting towers can be divided into four categories: synoptic wind, tornado wind, downdraft wind, and direct gust wind. All load cases are described in **Table A.3**. The IEC standard method was used for synoptic wind cases assuming a terrain category B and reference conditions of temperature and pressure. The "wind on all" was used to simulate all non-synoptic load cases. The tower drag coefficient of 1.6 used in the "wind on all" method is difficult to verify, but it seems acceptable considering that the wind speeds selected for the comparison are arbitrary values. Ideally this coefficient would be selected for each tower based on validated models or wind tunnel tests.

A gust wind speed of 70 m/s was used for all tornado loadings (see **Table A.3**) to match the upper limit of an F2 tornado or an EF3 tornado according to the enhanced Fujita scale. On the other hand, the gust wind velocity for downdraft loading is 50 m/s based on design wind speeds in the Australian standard (ENA, 2006). For the downdraft load cases, the wind pressure is also uniformly applied to the conductors. It is important to note that these load cases were selected to explore some possible reasonable approaches to design overhead lines against localized HIW. It is recommended that for the study of an actual line, specific wind speeds be chosen based on field observations, whenever available. Considering that current knowledge is limited on localized HIW effects on overhead lines, the "wind on all" method is deemed adequate as the reduced number of multiplying factors allows for a rational choice of the design wind speed. Hopefully, in a near future, a better localized HIW loading model and relevant wind speed data will become available. It will then be possible to improve the simplified load cases discussed herein.

In **Table A.3**, the "Synoptic 30 m/s – 0°" load case represents a typical synoptic wind load: the wind speed of 30 m/s in this case is a 10-minute average value. Other simulations at wind speeds of 35 m/s and 40 m/s were performed to be used as controls. The transverse direction (wind perpendicular to conductors) is used by default because it is the basic case.

Table A.3 – Summary of wind load cases					
Load case		Load case description	Wind model	Wind speed (m/s)	Wind direction (°)
1	Synoptic	Synoptic 30 m/s - 0°	IEC	30	0°
2		Synoptic 35 m/s - 0°	IEC	35	0°
3		Synoptic 40 m/s - 0°	IEC	40	0°
4		Synoptic 30 m/s > 15 m	IEC	30	0°
5	Tornado	Tornado full 0°	Wind on all	70	0°
6		Tornado full 15°	Wind on all	70	15°
7		Tornado full 45°	Wind on all	70	45°
8		Tornado full 90°	Wind on all	70	90°
9		Tornado below h_1	Wind on all	70	0°
10		Tornado lift	Wind on all	70	0°
11		Tornado BL profile	Wind on all	varies	0°
12		Tornado Wen profile	Wind on all	varies	0°
13	Downdraft	Downdraft full 0°	Wind on all	50	0°
14		Downdraft full 45°	Wind on all	50	45°
15		Downdraft full 90°	Wind on all	50	90°
16		Downdraft > 15 m	Wind on all	50	0°
17		Downdraft BL profile	Wind on all	varies	0°
18		Downdraft Wood profile	Wind on all	varies	0°
19		Direct gust wind	Wind on all	70	0°

All the tornado load cases studied neglect the wind forces on conductors as suggested by some authors (ASCE, 1991; Behncke and White, 1984; Behncke et al., 1994; Ishac and White, 1995). The "Tornado below h_1" load case is suggested to obtain the worst effect in the bracing members of self-supporting towers located below the centroid of the conductor loads. The height $\mathbf{h_1}$ is determined by the projected intersection of the main legs as shown in **Figure 11**. All the towers used in the simulations have only one bend line and therefore there is no value for $\mathbf{h_2}$. For the Canadian Bridge 0° tower, this load case does not exist since the projected leg intersection is located above the tower top. Load cases "Tornado 15°", "Tornado 45°" and "Tornado 90°" are the same as "Tornado full", except that they are applied in different directions. These variable directions were also tested for downdraft winds.

Downdraft load cases are more similar to synoptic load cases than tornado cases because wind is applied to both the supports and the conductors. "Downdraft above 15 m" matches a suggestion made in CIGRÉ TB 256 (2004). "Synoptic above 15 m" was also created in order to compare the synoptic wind method to the "wind on all" approach for this type of loading.

Additional load cases were defined to verify some of the assumptions made in the tornado and downdraft loadings. First, load case "Tornado lift" verifies the suggestion made in the ASCE Manual 74 (1991) that upward vertical winds during a tornado could be strong enough to lift conductors and therefore, the self-weight of conductors should be neglected for tornado loadings. The "Tornado lift" loading represents a strong uniform wind applied over the full height of the structure, but no wind nor gravity load are coming from the conductors.

Second, the assumption of not adjusting wind pressure with height for all tornado and downdraft load cases was verified. For tornadoes, two profiles were used: the boundary layer 1/7 power law described in Section 3.2.3 (Tornado BL profile), and a profile taken from the model by Wen (1975) (Tornado Wen profile) assuming a boundary layer thickness of 200 m. Wen's model is partially described in **Appendix B.2**. The profile derived from this model cannot be assumed to be typical of tornadoes as it is only one possibility among others. In effect, the profile varies greatly with the boundary layer thickness value, and with the location of the tower with respect to the centre of the tornado. In order to be able to compare the "Tornado BL profile" and the "Tornado Wen profile" with the "Tornado full" load case, the design wind speeds were selected such that the total wind force applied to the structure was the same for the three load cases. The three profiles are as shown in **Figure A.5**.

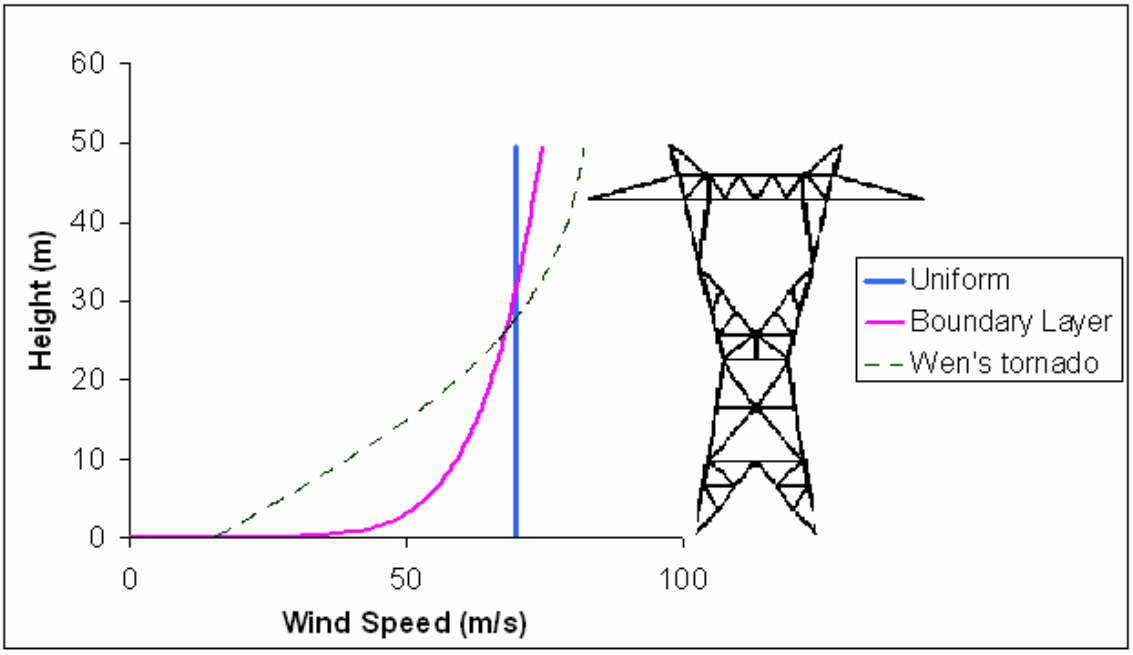

Figure A.5 - Horizontal tornado wind profiles for the CB0 tower

For downdrafts, the same boundary layer profile was used, as well as a profile given by Wood's formula (Wood *et al.*, 2001) assuming that the maximum wind speed occurs at an altitude of 50 m. Wood's formula is described in **Appendix B.1**. **Figure A.6** shows the profiles for the "Downdraft BL profile" and the "Downdraft Wood profile" load cases.

Whenever needed, the conductor gust response factor was also adjusted to make sure that the total wind force resultant was the same for all the load cases compared.

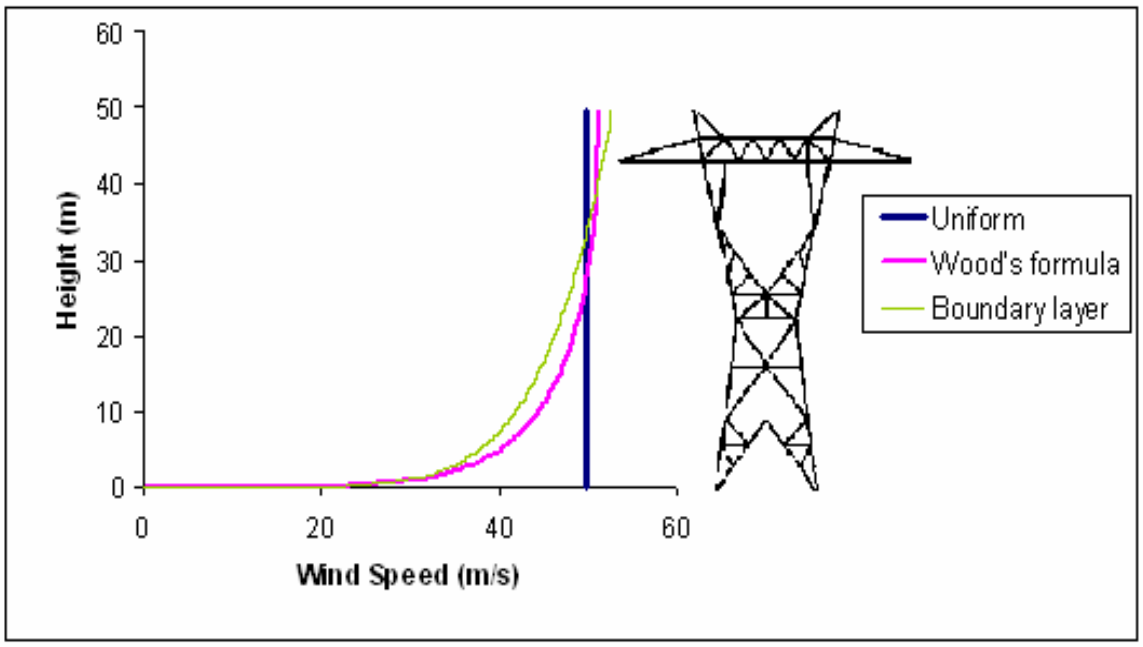

Figure A.6 - Horizontal downburst wind profiles for the CB0 tower

The last load case in **Table A.3** is the "Direct gust" loading. This case is based on the suggestion by Behncke and White (2006). For this loading, wind pressure is applied to the support and to part of the conductors. This "Direct gust" load case is applied to model the effects of an F2 tornado on both the conductors and the tower directly hit by the tornado. Hence, the wind speed is 70 m/s and the width of the gust is 160 m (80 m on each side of the support) as defined using the Fujita-Pearson scale (**Table 1**).

A.3 Results and discussion

This section shows and analyzes the effects of the various wind loadings described in **Appendix A.2** on the member forces in the four towers modelled. The relative variation of axial forces in the tower members for the various load cases is the focus of this discussion.

A.3.1 Results

To facilitate the analysis of results, only the following group of tower members are here examined:

- the main leg members below the waist;
- the transverse diagonal bracing members below the waist;
- the longitudinal diagonal bracing members below the waist.

Tables A.4 and A.5 below show for the four towers the relative compression force of the main leg and bracing members below the waist compared to the basic case (synoptic wind, 30 m/s, 0° or transverse).

A.3.2 Tables

Table A.4 - Relative compression forces for the Peabody/Wisconsin towers

Table A.4 - Relative compression forces for the Peabody/Wisconsin towers								
Load case		**Load case description**	**Ratio of the force (in %) for the loading case considered compared to the basic case of the transverse synoptic wind 30 m/s - 0°**					
			Peabody Tower			**Wisconsin tower**		
			Main leg	**Bracing member (1)**		**Main leg**	**Bracing member**	
				transv	**long**		**transv**	**long**
1	Synoptic	Synoptic 30 - 0°	100	100	100	100	100	100
2		Synoptic 35 - 0°	134	136	140	133	132	134
3		Synoptic 40 - 0°	173	177	185	171	169	172
4		Synoptic 30 > 15 m	103	73	101	87	91	101
5	Tornado	Tornado full 0°	114	531	86	121	176	79
6		Tornado full 45°	165	476	243	176	203	285
7		Tornado full 90°	139	235	268	147	93	276
8		Tornado below h_1	70	579	17	95	192	31
9		Tornado lift	110	531	90	117	181	76
10		Tornado BL profile	119	498	95	126	184	87
11		Tornado Wen profile	132	399	119	140	198	108
12	Downdraft	Downdraft full 0°	150	164	163	151	164	146
13		Downdraft full 15°	156	236	160	156	192	174
14		Downdraft full 45°	127	218	138	135	151	197
15		Downdraft full 90°	75	111	137	79	53	140
16		Downdraft > 15 m	150	96	159	129	144	134
17		Downdraft BL profile	155	140	168	154	167	151
18		Downdraft Wood profile	155	142	168	154	168	151
19		Direct gust wind	176	446	185	187	236	157
(1) tension forces instead of compression forces as the tension-only assumption has been applied in the calculation of the Peabody tower								

Table A.5 - Relative compression forces for the Canadian Bridge towers

Table A.5 - Relative compression forces for the Canadian Bridge towers								
Load case		Load case description	Ratio of the force (in %) for the loading case considered compared to the basic case of the transverse synoptic wind 30 m/s - 0°					
			CB0			CB15		
			Main leg	Bracing member		Main leg	Bracing member	
				transv	long		transv	long
1	Synoptic	Synoptic 30 - 0°	100	100	100	100	100	100
2		Synoptic 35 - 0°	131	122	134	127	122	125
3		Synoptic 40 - 0°	168	147	172	157	147	155
4		Synoptic 30 > 15 m	100	96	100	96	83	96
5	Tornado	Tornado full 0°	99	141	97	118	153	122
6		Tornado full 45°	155	231	175	162	265	223
7		Tornado full 90°	132	111	155	127	210	227
8		Tornado below h_1	NA	NA	NA	NA	NA	NA
9		Tornado lift	93	132	91	112	143	117
10		Tornado BL profile	106	146	102	125	153	128
11		Tornado Wen profile	120	155	114	139	151	140
12	Downdraft	Downdraft full 0°	138	131	139	147	139	146
13		Downdraft full 15°	145	148	151	154	153	166
14		Downdraft full 45°	124	156	134	130	193	155
15		Downdraft full 90°	77	112	89	77	124	130
16		Downdraft > 15 m	138	126	138	141	80	137
17		Downdraft BL profile	143	132	144	150	140	149
18		Downdraft Wood profile	142	132	144	150	140	149
19		Direct gust wind	109	144	108	162	178	164

A.4 Comparison of tower response to local cases and discussions

Dividing tower members into groups allowed rapid identification of the critical load cases. Each of the following subsections discusses the results of a small number of load cases.

A.4.1 Synoptic wind versus tornado loading

This first group of load cases discussed is composed of “Synoptic 30 m/s”, “Tornado full”, and “Tornado below h_1”. Despite their different wind speeds and loading models, it

is interesting to compare results of the tornado load cases and the traditional synoptic load case to identify which members might need to be reinforced to sustain such tornado loadings.

Compared to "Synoptic 30 m/s", "Tornado full", which applies a much higher total force on the system, creates similar (CB0) or larger (PB, WI and CB15) forces in the main legs. As expected, for "Tornado below h_1", the forces in the main leg members drop significantly. Most critical members for the tornado load cases are bracing members located in the lower portion of the towers. Some of them undergo very large increases in axial force and would certainly need to be changed or reinforced to resist localized HIW effects.

A.4.2 Varying direction of tornado loading

This section compares axial forces for tornado loadings over the full height of the structure applied in various directions. The "Tornado full" load case, which is in the transverse direction, and other load cases varying from 0° to 90° with respect to the transverse axis of the tower are analyzed to identify the critical directions for tornado loadings.

A first observation is that the total wind force on the structure only is higher for the longitudinal load case (90°) than for the transverse load case (0°) since there is more drag area in the longitudinal faces of all the towers studied. This is typical of self-supporting towers with transverse cross-arms. However, the difference in total wind force for longitudinal and transverse loadings is small, and the longitudinal load case is not critical for all members. The total wind force on the structure only is highest for 45° without cross-arms and more than 45° with transverse cross-arms.

The critical wind direction for a given member mostly depends on the member position in the tower. The loading is critical at an angle of nearly 45° for the main legs. If changes are required to the foundations due to the very high tornado total wind force, the consideration of this loading could be very costly. It should be emphasized that the tornado wind speed of 70 m/s selected for these simulations is very high: in most regions, a lower tornado design wind speed is appropriate. In this context, increasing the overall reliability of towers at low cost will be possible if the necessary design changes are limited to diagonal bracing members. However, the simplified tornado loading suggested only covers for the situation where an extremely narrow horizontal wind force is applied to the structure. The decision to consider severe tornado loads in design must be justified either by a history of tornado-related line failures in the region, or by successful tornado-resistant design practices in other regions with similar climates.

As expected, transverse bracing members take generally higher wind forces when the wind is applied transversally, whereas longitudinal bracing members are often critical for wind applied longitudinally (for the load case "Tornado 90°") or nearly longitudinal. It is therefore crucial to apply the tornado load case in a number of directions. Based on the

towers studied, it would seem reasonable for example to apply a tornado load case in three different directions: transversally, at 45°, and longitudinally. This should cover critical loads for all the members.

Varying the wind direction of tornado loading has nearly the same consequences as varying the direction of the synoptic wind on the tower only as presented in **Appendix C2.**

A.4.3 Synoptic loading versus downdraft loading

This section compares synoptic loadings of 30, 35 and 40 m/s to the following three downdraft load cases: “Downdraft full” and “Downdraft above 15 m”. Both the synoptic and downdraft loadings are applied to the conductors and the supports. The fundamental difference between the proposed downdraft loadings and the synoptic wind loadings is that the design wind speed for downdrafts is converted to horizontal pressures without the application of gust response factors and height adjustment associated with boundary layer winds. This section also includes comments on the “Synoptic 30 m/s above 15 m” load case, which allows direct comparison with the “Synoptic 30 m/s” load case.

The “Downdraft full” load case is nearly equivalent to a severe synoptic load case in terms of the distribution of axial forces. For the Wisconsin tower, the relative compression force is slightly lower for “Downdraft full” compared to “Synoptic 40” in the member groups compared. Among all downdraft loadings studied, “Downdraft full” yields higher relative compression forces in most members for all four towers. The forces in the members above 15 m are similar for the “Downdraft above 15 m” and the “Downdraft full” load cases. However, in most of the members located in the bottom part of the tower, the axial forces are significantly higher for “Downdraft full”. Similarly, the “Synoptic 30” load case is more critical than “Synoptic above 15 m” for most of the tower members below 15 m.

The “Downdraft above 15 m” does not change all axial forces enough to be considered as a design load case. Applying wind on the full structure for downdrafts seems more reasonable considering the current knowledge on wind field models of downdrafts. However, the load path is the same for the “Downdraft full” and synoptic loadings. Hence, “Downdraft full” might not be relevant since synoptic load cases are already applied to the tower. A valid option is to use a similar procedure for downdraft winds and synoptic winds, as suggested in the Australian standards (ENA, 2006), while using design wind speeds from separate statistical databases. The disadvantage of this approach is that most of the factors derived for the synoptic wind procedure do not apply to downdraft winds. Also, for codes such as the IEC 60826 (2003), where the averaging period of wind speeds is 10 minutes, it is difficult for the designer to select rationally a downdraft design wind speed. In most instances, only a few downdraft records or damage analyses are available, even for regions where downdrafts frequently occur. Until more knowledge is available on the effect of downdrafts on overhead lines, the “Downdraft full” load case is deemed adequate to complement the synoptic wind loading.

A.4.4 Varying direction of downdraft loading

The “Downdraft full” load case was compared to equivalent loads applied at angles varying from 0° to 90° with respect to the transverse axis. It is observed that the relative compression force of members decreases with increasing angles for most members, except for small angles. This is due to the wind force on the conductors which is very high for transverse wind, but negligible for longitudinal wind. Hence, the “Downdraft full” and the “Downdraft 15°” load cases govern for a large majority of the members in all four towers. The most critical direction for the main legs is nearly 15°. However, a number of bracing members in the longitudinal face are critical under “Downdraft 90°”. The results indicate that for downdraft loadings, the assumption that transverse wind is the governing load case is not always valid. The same warning could be made for synoptic wind loading, especially for tangent towers.

Overall, even though the downdraft loading applied transversally is critical for most members, the direction of this load case should still be varied. As proposed for tornado loading, the downdraft loading can be applied at 0°, 15°, 45° and 90° to ensure all members can resist such conditions.

Varying the wind direction of downdraft loading has nearly the same consequences as varying the direction of the synoptic wind on the tower equipped with conductors as presented in **Appendix C2**.

A.4.5 Neglecting the self-weight of conductors in tornado loading

The “Tornado full” load case was compared to “Tornado lift” to investigate the effect of neglecting the self-weight of conductors in tornado loadings. This test was based on the suggestion made in the ASCE Manual 74 (1991) that conductors could be lifted due to large upward wind forces produced in tornadoes. For a Cardinal conductor with a length of 175 m (half the wind span of the Peabody tower), this uplift represents a vertical wind force of more than 3 kN. The tornado wind field model and the parameters for a severe tornado (F3) presented by Wen (1975) were used to perform simple calculations of upward forces during tornadoes. Assuming the tornado is centred at the support, the wind force over 175 m for that particular event is lower than 2 kN. Therefore, it is unlikely that the upward forces during a tornado are large enough to compensate for the whole self-weight of conductors. Moreover, the simulations indicate that most members have slightly higher loads under the “Tornado full” load case where the weight of conductors is not neglected than for the “Tornado lift” load case.

In all, the “Tornado lift” load case does not need to be applied since conductors are unlikely to be completely lifted, and it is not more critical than the “Tornado full” load case for self-supporting towers. Nevertheless, “Tornado lift” can be critical for the uplift strength of foundations.

A.4.6 Varying wind profile of tornado loading

The "Tornado full" loading was compared to the "Tornado BL profile" and "Tornado Wen profile" load cases to verify whether the assumption of a uniform wind profile is adequate for tornado loadings. The comparison is relevant since the total wind force is equivalent for these three load cases. The most severe case for the top portion of the towers is the "Tornado Wen profile". This load case is probably not representative of all tornado events, but the results are still useful to assess the effect of wind profile changes on the axial forces within tower members.

For most members, the "Tornado Wen profile" load case produces larger forces in the tower members. However, some bracing members have higher forces under the "Tornado full" load case. This is particularly true for the bracing members in the bottom part of the towers. This illustrates the same concept mentioned in Section 5.3 where synoptic and tornado loadings are compared: when the resultant wind force on the tower is located at a lower height, the lower bracing components receive larger loads and the main members receive smaller loads. Therefore, applying a uniform tornado wind pressure with height underestimates the forces in the main leg members and overestimates the forces in the bracing members. This may turn out to be a good design compromise as the main leg members are likely to be governed by other loads than tornadoes.

To obtain the same total wind force for the "Tornado Wen profile" as for the "Tornado full" load case, a very high wind speed was applied at the top of the tower (over 80 m/s for the CB0 tower). This wind speed could only be produced in very severe tornadoes and hence, the importance of underestimating the main member forces in "Tornado full" is limited. Therefore, unless better load modeling is possible with the availability of detailed tornado parameters for a region, the uniform profile of wind is adequate for tornado loadings.

A.4.7 Varying wind profile of downdraft loading

In this section, the effects of changing the wind profile for downdraft loadings were studied. As for profile changes in tornado loadings (see previous section), the forces in the main leg members and the bracings depend on the location of the resultant wind force. The profile from Wood *et al.* (2001) is similar to the boundary layer profile, but has slightly more wind pressure at low altitude. Hence, axial forces are higher in the main leg members for the "Downdraft BL profile" load case and are higher in the transverse bracing members below the waist for the "Downdraft full" load case. The choice of the wind profile has less impact on the axial forces for downdraft loadings than for tornado loadings.

From these results, a uniform profile of wind seems adequate for downdraft loadings. The profile suggested by Wood *et al.* (2001) could be interesting after further validation. However, the main characteristic of this profile is its high wind speed at low altitude, and therefore a simpler uniform profile can produce realistic results.

A.4.8 Direct gust wind loading

This last HIW load case is very severe because the 70 m/s wind speed of the tornado load cases is applied not only to the structure but also to part of the conductors over a width of 160 m. These values of wind speed and path width correspond to the upper limits of the F2 tornado.

In terms of the loading paths, the "Direct gust" load case is an intermediate between a severe synoptic wind load case ("Synoptic 40 m/s") and a tornado loading ("Tornado full"). An important advantage of the "Direct gust" wind loading method as proposed in Behncke and White (2006) is that the designer can make a rational decision for the wind speed to apply to the system. This approach eliminates the problem of extrapolating from incomplete statistical data and does not rely on complex wind models that might not apply to the type of gust winds encountered in the region of the line. However, with this method, one could easily apply unrealistically large forces to the system if the wind speeds are too large. The most difficult parameter to evaluate is the path width of the wind storm.

A.5 Conclusions

A number of simplified load cases to account for localized HIW on overhead transmission lines were discussed. The tornado loading proposed by some authors and consisting of applying a strong uniform horizontal wind pressure on the full height of the tower and no pressure on the conductors is critical for the bracing system of self-supporting towers. The loading needs to be applied in a number of different directions including the transverse and longitudinal directions in order to identify the critical members. The suggestion of the ASCE Manual 74 to neglect the self-weight of conductors for this loading has little effect on the axial forces for the four towers studied and its implementation is not recommended if there is no impact on the uplift of the foundations. Therefore, the final recommendation for the tornado loading cases is to consider a uniform horizontal wind speed profile in at least three orientations (longitudinal, transverse, and oblique at 45°) with conductor self-weight and tension. The wind is considered on the tower only and the resulting pressure load is calculated with a drag factor appropriate to the tower geometry. Wind speeds corresponding to an F2 tornado (maximum wind speed between 50 and 70 m/s) are appropriate for this tornado loading in the regions affected by this type of storm. This load case needs further validation through analysis of tower failures under tornadoes.

Severe downdrafts apply high wind pressures to both the line supports and the conductors. The approach of the Australian standards (ENA 2006) is deemed adequate in the absence of validated loading models specific to downdrafts. It consists of using the conventional wind loading calculation procedure with design wind speeds based on

specific statistical analysis of downdrafts rather than derived from synoptic wind observations. Another possible option is to use a uniform horizontal wind speed applied to both the conductors and the support, without adjustment with height: this allows the designer to make a rational decision on the downdraft design wind speed in the case that limited information on previous downdraft events is available. Like tornado loadings, downdraft loadings should also be applied in several directions to identify critical members.

The scope of the study had to be limited and the analysis was restricted to self-supporting towers. It would also be interesting to study the effect of HIW loadings on guyed structures of various geometries where the lattice masts always actively participate in the resistance to lateral loads, unlike the main legs in self-supporting lattice towers.

Another important limitation in the study was that the knowledge available on the wind flow during downdrafts is still limited compared to the knowledge on tornadoes or synoptic winds. As mentioned earlier, the linear analyses performed in this study do not represent accurately the behaviour of lattice towers under failure conditions. Nonlinear analyses could give more details on the effect of HIW on particular transmission structures. More importantly, future work should include the participation of utilities. The load cases need to be applied on specific towers in a particular region. Only the utilities can judge on how useful HIW load cases can be for their structures.

For transmission line engineers, the first step towards dealing properly with localized HIW effects is to recognize that present design codes and their traditional wind loading methods do not cover such localized storms. Next, it is important that the statistical analysis of downdraft, tornado, and synoptic wind events be done separately for a rational reliability-based design approach. In the absence of statistically significant observations, deterministic values of wind speeds may be selected which reflect the vulnerability of the area to a credible extreme storm. Changes to wind design practices may become necessary only if a genuine hazard of localized HIW storms is identified. Otherwise, the traditional synoptic wind design approach is sufficient. Extensive and costly mitigation on existing overhead line supports may be difficult to justify considering the many uncertainties and limited knowledge on the effects of localized HIW storms, whereas design of new lines can more easily integrate HIW-resistant load cases.

When the hazard is real and its mitigation impractical, security measures can be implemented in order to reduce the risk of cascading failures following the collapse of a support and to ensure rapid recovery of the network.

B. Wind profile models

B.1 Wood's empirical formula

Wood's formula (Wood *et al.*, 2001) for downdrafts was obtained from mean velocity measurements at various distances of a jet of air impinging on a vertical surface. The wind velocity profile (see Figure 4) resulting from this formula is normalized with respect to the peak mean velocity, whereas the height is normalized with respect to the height where the velocity is equal to half its maximum value.

$$V/V_{max} = 1.55 (z / \delta)^{1/6} [1 - erf (0.70 z / \delta)],$$

where:

V the mean velocity (m/s) at height above ground z (m)

V_{max} the peak mean velocity (m/s)

δ the height where the velocity is equal to half its maximum value (m)

erf the error function (-)

For the numerical study reported in **Appendix A**, δ is equal to 270 m, resulting in a peak mean velocity located at 50 m above ground. The value of V_{max} was chosen to make the total wind force resultant of the "Downdraft Wood profile" and "Downdraft full" load cases equal (see **Appendix A.2**). V_{max} ranges between 51.3 and 52.2 m/s for the various towers.

B.2 Wen's model

Wen's tornado model (Wen, 1975) divides the tornado wind speed into tangential, radial, and vertical components (see **Figure 5**). For the purpose of our study, only the tangential component (T) was used.

Above the boundary layer:

$$T = 1.4\ V_{max} / \rho\ [1 - \exp(-1.259\ \rho^2)]$$

Within the boundary layer:

$$T = 1.4\ V_{max} / \rho\ [1 - \exp(-1.259\ \rho^2)] * [\ 1 - \exp(-\pi\ n\ )] * \cos(\ 2\ b\ \pi\ n\ )$$

$$\rho = r / r_{max}$$

$$n = z / \delta$$

$$\delta = \delta_0\ [1 - \exp(-0.5\ \rho^2)]$$

$$b = 1.2 \exp(0.8\ \rho^4)$$

where:

T the tangential velocity (m/s) at a given height above ground z (m) and distance from the centre of the tornado vortex r (m)

V_{max} the maximum tangential velocity above the boundary layer (m/s)

r_{max} the core radius of the tornado vortex (m)

δ_0 the boundary layer thickness (m)

The profile shown in **Figure A.5** would be located at $r = r_{max}$ and considers some translational velocity of the tornado. The boundary layer thickness, δ_0, is equal to 200 m, r_{max} is equal to 30 m, and V_{max} was originally taken as 45 m/s. After adding a translation velocity of about 10 m/s to the tangential velocity calculated, the profile was scaled to make the total wind force resultant of the "Tornado Wen profile" and "Tornado full" load cases equal.

The choice of the parameters may influence the profile. For this study, they were chosen to the best knowledge of the author to match an F2 or F3 tornado. Therefore, the profile shown is only one possible profile among others. It was beyond the scope of this study to develop accurate tornado profiles.

C. Influence of direction and height of wind load on forces in tower members

C.1 Influence of height of wind load on member forces

The influence of the height of the resultant wind load on the bracing members and main legs is summarized in **Table C.1.**

Table C.1 - Influence of height of wind load on the magnitude of axial forces in members of a tangent tower

Height h of horizontal wind load on tower or conductor		Members in the tangent tower	
		Bracing member	Main leg
Above height h_1	$h > h_1$	$-\lvert h - h_1 \rvert$	$\lvert h - h_0 \rvert$
At height h_1	$h = h_1$	0	
Below height h_1 and above height h_0	$h < h_1$	$+\lvert h - h_1 \rvert$	
	$h > h_0$		
At height h_0	$h = h_0$	0 or $+\lvert h - h_1 \rvert$ (1)	0
Below h_0	$h < h_0$	0	0
(1) 0 or $+\lvert h - h_1 \rvert$ depending on the type of bracing (X, V or Λ)			
h = height of horizontal wind load considered h_0 = height of intersection point of bracing (diagonal) members h_1 = height of intersection point of main legs (See **Figure 11 a**)			

The horizontal component of the axial force in the bracing member of a statically determinate tangent lattice tower is proportional to the resultant wind load (above the bracing) at height h and its lever arm $|h - h_1|$ (positive or negative) with regard to the intersection point of the main legs at height h_1 (**Figure 11 a**).

The intersection of the main legs is usually selected to coincide nearly with the horizontal resultant of the synoptic wind load in order to minimize the stresses in the bracing members between the main tower legs. Generally the resultant of the wind loads on conductors is situated above the intersection point and the resultant of the wind loads on the tower below. Wind loads above and below height h_1 of the intersection of the main legs have an opposite effect on the bracing member. It means that the axial force in the bracing member due to the wind load on the tower is compensated by the effect of the wind load on conductors.

Generally, the bracing members could be overstressed if the resultant wind load is lowered below the height h_1 of the intersection of the main legs. This happens if:

- A uniform wind speed will be considered, such as in the case of downdrafts and tornadoes;

- The wind load on the conductors is neglected, such as in the case of tornadoes.

The axial force in the main leg is proportional to the resultant wind load at height h and its lever arm $|h - h_0|$ (positive) with regard to the intersection point of its bracing members at height h_0.

In contradiction with the bracing members, the axial forces in the main legs will decrease as the resultant wind load of the downdraft and the tornado will be lowered.

If the bracing members of the lattice tower are not statically determinate but rather indeterminate, the conclusions may be somewhat different, especially for the bracing members.

C.2 Critical direction of wind load for forces in members

The influence of the wind direction φ on the axial forces of the main leg and the bracing members is summarized in **Table C.2** below.

Table C.2 Influence of wind direction φ on axial forces in members of a tangent tower

Tower member	Wind load on	Wind type	Wind direction φ						
			0°	>0° ~15°	> 0° ~20°	45°	>45° ~50°	<90° ~75°	90°
Leg member	Tower without crossarms	-	A=Min	↑	↑	Max	↓	↓	A=Min
	Tower with crossarms	Tornado	A=Min	↑	↑	↑	Max	↓	B>A
	Conductors	-	Max	↓	↓	↓	↓	↓	0
	Total	Synoptic	↑	Max	↓	↓	↓	↓	↓
		Downdr.	↑	↑	Max	↓	↓	↓	↓
Transv. bracing	Tower	Tornado	↑	Max	↓	↓	↓	↓	0
	Conductors	-	Max	↓	↓	↓	↓	↓	0
	Total	Synoptic	↑	Max(1)	↓	↓	↓	↓	0
		Downdr.	↑	Max(1)	↓	↓	↓	↓	0
Longit. bracing	Tower	Tornado	0	↑	↑	↑	↑	Max	↓
	Conductors	-	0	0	0	0	0	0	0
	Total	Synoptic	0	↑	↑	↑	↑	Max	↓
		Downdr.	0	↑	↑	↑	↑	Max	↓

(1) For the transversal bracing the effect of the wind load on the tower and conductors are opposite so that the critical angle varies from one case to another.
Note - Angles of 15°, 20°, 50° and 75° are only indicative and very approximate.

The arrows in **Table C.2** indicate an increasing or decreasing value of axial force as the angle φ is further increased.

We recall that the maximum value of the axial forces both in the transverse and longitudinal bracings is very low as the resultant synoptic wind load nearly coincides with the intersection point of the main legs. The maximum value for the downdraft is much higher.

Table C.3 has been established based on **Table C.2**.

Table C.3 - Critical direction φ of wind load for forces in members of tangent tower

Wind type	**Synoptic wind**				**Localized HIW**	
Members in the tangent tower	**Tower without cross-arms**	**Tower with cross-arms**	**Conductor only**	**Total: tower and conductor**	**Downdraft (wind on tower and conductor)**	**Tornado (wind on tower only)**
Main leg	45°	> 45° (~ 50°)	0°	> 0° (~ 15°)	> 0° (~ 20°)	> 45° (~ 50°)
Transverse bracing	> 0°	> 0°	0°	> 0°	> 0°	> 0°
Longitudinal bracing	< 90°	< 90°	NA	< 90°	< 90°	< 90°

0° = transversal direction (perpendicular to the conductors)
45° = oblique direction
90° = longitudinal direction (parallel to the conductors)
Note: Angles of 15°, 20° and 50° are only indicative and very approximations

The most critical synoptic wind direction on a tangent lattice tower with statically determinate bracing panels is:

- 45° for the main leg of a symmetrical tower without cross-arms (column 2 in Table C.3) ;
- Slightly more than 45° (~ 50°) for the main leg of a tower with cross-arms in the transversal direction, but without conductors, since the area of the cross-arms seen by the longitudinal wind is larger than the area seen by the transversal wind (column 3 in Table C.3);
- 0° if only the wind load on the conductors is considered. Only the perpendicular component of the wind load on the conductor is effective (at least if the sag is neglected in comparison with the wind span) (column 4 in Table C.3);
- Somewhat greater than 0° (~ 15° to 30°) for the combined effect of tower and conductors depending on their relative importance (column 5 in Table C.3);
- 0° (transversal) for the bracing members in the transversal face of the tower;
- 90° (longitudinal) for the bracing members in the longitudinal face of the tower.

For the tornado, the most critical wind direction for all members is identical to the case of the synoptic wind loading on the tower only without any conductors (column 3 in Table C.3).

For the downdraft, the angle of the most critical wind direction for the leg member and the longitudinal bracing is similar to the case of combined synoptic wind loading on both the tower and the conductors (column 5 in Table C.3). As the impact of the wind loading on the tower is higher for the downdraft, the critical angle can be higher for the leg member. However, for the transversal bracing the impact of the wind load on the tower and conductors are opposite so that the critical angle varies from one case to another.

If the bracing members of the lattice tower are not statically determinate but rather indeterminate, the conclusions may be somewhat different, especially for the bracing members.